

**TRANSCRIPTIONAL ANALYSIS OF THE UNFOLDED PROTEIN
RESPONSE (UPR) AND LYMPHOMA MICROENVIRONMENT DURING
MAREK'S DISEASE VIRUS (MDV) INFECTION**

by

Sabarinath Neerukonda

A thesis submitted to the Faculty of the University of Delaware in partial fulfillment of the requirements for the degree of Master of Science in Animal Science

Fall 2015

© 2015 Sabarinath Neerukonda
All Rights Reserved

ProQuest Number: 10014918

All rights reserved

INFORMATION TO ALL USERS

The quality of this reproduction is dependent upon the quality of the copy submitted.

In the unlikely event that the author did not send a complete manuscript and there are missing pages, these will be noted. Also, if material had to be removed, a note will indicate the deletion.



ProQuest 10014918

Published by ProQuest LLC (2016). Copyright of the Dissertation is held by the Author.

All rights reserved.

This work is protected against unauthorized copying under Title 17, United States Code
Microform Edition © ProQuest LLC.

ProQuest LLC.
789 East Eisenhower Parkway
P.O. Box 1346
Ann Arbor, MI 48106 - 1346

**TRANSCRIPTIONAL ANALYSIS OF THE UNFOLDED PROTEIN
RESPONSE (UPR) AND LYMPHOMA MICROENVIRONMENT DURING
MAREK'S DISEASE VIRUS (MDV) INFECTION**

by

Sabarinath Neerukonda

Approved: _____
Mark S. Parcels, Ph.D.
Professor in charge of thesis on behalf of the Advisory Committee

Approved: _____
Limin Kung, Jr., Ph.D.
Chair of the Department of Animal and Food Sciences

Approved: _____
Mark W. Rieger, Ph.D.
Dean of the College of Agriculture and Natural Resources

Approved: _____
James G. Richards, Ph.D.
Vice Provost for Graduate and Professional Education

ACKNOWLEDGMENTS

Firstly, I would like to thank my advisor Dr. Mark S. Parcells for his invaluable mentorship, encouragement and support. I would also like to thank Dr. Serguei P. Golovan and members of my graduate advisory committee for their crucial guidance over the course of my graduate study. I would like to acknowledge all the members of Parcells and Golovan lab, whomever else I had a wonderful pleasure of working with, for their guidance and technical assistance. Finally, I would like to thank my family and friends.

TABLE OF CONTENTS

LIST OF TABLES	vi
LIST OF FIGURES	vii
ABSTRACT	ix

Chapter

1	INTRODUCTION	1
1.1	Marek's Disease	1
1.2	Marek's Disease Virus (MDV1):	2
1.3	Three Serotypes of MDV	2
1.4	MDV Pathogenesis:	3
1.4.1	Early Cytolytic Phase:	4
1.4.2	Latent Phase:	5
1.4.3	Secondary Cytolytic Phase:	6
1.4.4	Phase of Transformation:	6
1.4.4.1	The <i>meq</i> Oncogene	7
2	EVALUATION AND VALIDATION OF REFERENCE GENE STABILITY DURING MAREK'S DISEASE VIRUS INFECTION	11
2.1	Introduction	11
2.2	Materials and Methods	15
2.2.1	Cells and Viruses:	15
2.2.2	<i>In vivo</i> Tumor Collection:	15
2.2.3	Quantitative RT-PCR Analysis:	16
2.2.4	Primer Design:	17
2.3	Results	17
2.4	Discussion	22
3	INDUCTION OF THE UNFOLDED PROTEIN RESPONSE (UPR) DURING MAREK'S DISEASE VIRUS (MDV) INFECTION	25
3.1	Endoplasmic Reticulum:	25

3.2	ER Stress and The Unfolded Protein Response (UPR):.....	26
3.2.1	Inositol-1 Requiring Kinase (IRE1) Signaling:.....	27
3.2.2	PERK Signaling.....	28
3.2.3	Activating Transcription Factor 6 (ATF6) Signaling:.....	30
3.2.4	UPR and Innate Immunity.....	32
3.3	Herpesviruses and UPR.....	33
3.4	UPR Role in Tumorigenesis:.....	36
3.5	Hypothesis of Research:.....	38
3.6	Materials and Methods:.....	39
3.6.1	Cells and Viruses:.....	39
3.6.2	<i>In vivo</i> Tumor Collection:.....	40
3.6.3	Quantitative RT-PCR Analysis:.....	42
3.6.4	Primer Design:.....	42
3.6.5	Statistical Analysis:.....	43
3.7	Results and Discussion.....	44
3.7.1	UPR Induction in MDV-infected CEFs.....	44
3.7.2	UPR Induction <i>in vivo</i> in TK-Induced Lymphomas.....	54
4	CYTOKINE COMPOSITION OF TK INDUCED SOLID LYMPHOMAS...	61
4.1	Introduction:.....	61
4.2	Hypothesis of Research:.....	62
4.3	Materials and Methods:.....	63
4.4	Cytokine Profiling of TK Induced Lymphomas.....	63
	REFERENCES.....	70
	Appendix	
A	ALIGNMENT OF XBP1 SEQUENCES OF DIFFERENT SPECIES.....	86
B	PRIMER SEQUENCES USED IN THE STUDY.....	87
C	ANIMAL CARE AND USE COMPLIANCE.....	88

LIST OF TABLES

Table 2.1:	Bestkeeper analysis of housekeeping genes showing variation in gene expression.....	18
Table 2.2:	Pairwise correlation analyses between reference genes and bestkeeper index.	19

LIST OF FIGURES

Figure 2.1: Graph representing best keeper analysis of stability in their order of ranking from least stable to most stable.	19
Figure 2.2: Graph representing best keeper analysis of stability in their order of ranking from least stable to most stable.	20
Figure 2.3: Graph representing best keeper analysis of stability in their order of ranking from least stable to most stable..	21
Figure 2.4: Graph representing Normfinder analysis of stability in their order of ranking from least stable to most stable..	22
Figure 3.1: Schematic illustration of UPR Signaling Pathways.	31
Figure 3.2: XBP1 Splicing.	31
Figure 3.3: Solid white lymphoma mass (highlighted in blue square) and adjacent red non-lymphoma tissue (white square) dissected from the same spleen.	41
Figure 3.4: Relative expression of ATF4 in CU-2 infected CEFs..	46
Figure 3.5: Relative expression of GRP78/BiP in CU-2 infected CEFs.....	47
Figure 3.6: Relative expression of GRP94 in CU-2 infected CEFs.....	47
Figure 3.7: Relative expression of spliced XBP1(s) in CU-2 infected CEFs..	48
Figure 3.8: Relative expression of EDEM in CU-2 infected CEFs..	48
Figure 3.9: Relative expression of unspliced XBP1(u) in CU-2 infected CEFs.....	49
Figure 3.10:Relative expression of ATF4 among MDV1 pathotypes and vaccine strain..	51
Figure 3.11:Relative expression of BiP/GRP78 among MDV1 pathotypes and vaccine strains..	52

Figure 3.12:Relative expression of GRP94 among MDV1 pathotypes and vaccine strains.....	52
Figure 3.13:Relative expression of XBP1(s) among MDV1 pathotypes and vaccine strains.....	53
Figure 3.14:Relative expression of EDEM among MDV1 pathotypes and vaccine strains.....	53
Figure 3.15:Relative expression of UPR target genes in TK induced lymphoma..	60
Figure 4.1: Relative expression of T-helper cell signature cytokines and transcription factors in TK lymphomas.....	69
Figure A1: Above figure shows alignment of XBP1 genomic sequences from different species (Xenopus leavis, Danio rerio, Mus musculus, Gallus gallus, Bos Taurus and Homo sapiens) using laser gene software. A 26nt spliced fragment is indicated by dotted line from nucleotide positions 1205-1320.	86

ABSTRACT

Marek's disease virus (MDV) is a highly cell-associated alphaherpesvirus, capable of replicating in multiple cell types (B cells, T cells, macrophages, epithelial and fibroblast cells) and specifically transforming activated CD4⁺ T helper cells, polarizing them into a T regulatory (T_{REG})-like immunophenotype. Marek's disease (MD) is caused by MDV and is one of the most prevalent diseases in poultry production, worldwide. MDV is associated with profound immune suppression and the rapid formation of T cell lymphomas.

Real time RT-PCR is widely used in the field of MD research to measure transcriptional responses to infection and/or vaccination. Studies in the past have either used cellular β -actin or GAPDH as internal reference genes, although the stability of their expression in the context of MD infection was never investigated. We investigated the suitability of five housekeeping genes (β -actin, 28S RNA, 18S RNA, GAPDH, Peptidyl-prolyl-isomerase B aka cyclophilin B or PPIB) as standard internal controls during lytic infection *in vitro* in CEFs and latent infection *in vivo* in TK strain-induced tumors. Upon Bestkeeper[®] and Normfinder[®] analysis of stability, we found that β -actin is the least stable reference gene, while both PPIB and 28S RNA displayed equally higher stability in the context of MD infection both *in vitro* and *in vivo*.

MDV serves as an excellent model to study how herpesvirus lytic replication triggers cellular stress activation and how the virus modifies the malefic consequences

of cellular stress (translation attenuation, ERAD and apoptosis) while allowing beneficial effects (chaperone induction) that support viral replication.

In a preliminary study, we investigated the induction of ER stress and activation of the unfolded protein response pathways (UPR) during the course of MDV1 (mildly virulent CU-2) lytic replication in CEFs. We observed a lack of induction of UPR signaling until day 4 post-infection, suggesting that UPR signaling was maintained in a repressed state during this initial phase of infection. However by day 5, we observed a significant transcriptional induction of ATF6 (GRP78/BiP) and IRE1 (XBP_(S)) pathways while the PERK (ATF4) pathway was still maintained in a repressive state. Based on the transcriptional responses observed on day 5 with mildly virulent CU-2, we followed up our investigation with MDV1 pathotypes of higher virulence, RB1B (very virulent), MD5 (very virulent) and TKING (very virulent plus). Among the different MDV pathotypes, the vv+ MDV strain (TK) induced the highest level of UPR gene expression compared to other pathotypes at 5 days post-infection, despite a more limited replication in these cells (typically, vv+MDVs, require adaptation or a higher number of passages to replicate in CEF). UPR induction seen in vvMDV (RB1B and MD5) infection is relatively lower than that of vv+MDV infected cells indicating that UPR pathways might be more tightly regulated by vvMDVs.

Tumor cells are subjected to severe conditions such as hypoxia, glucose deprivation, proto-oncogene activation, rapid proliferation and increased cytokine secretion. Each of these is capable of inducing ER stress and UPR activation in the cancer cells. UPR plays a paradoxical role in tumor cells and the tumor microenvironment, either promoting adaptation and cell survival under acute stress, or triggering apoptosis upon failure of adaptation and chronic ER stress. However, many

tumor cells also possess the ability to block apoptosis under chronic ER stress. Prolonged activation of PERK (Protein kinase R-like ER Kinase) and IRE1-JNK (Inositol requiring kinase 1- Jun N terminal Kinase) pathways induce apoptosis while IRE1-XBP1(s) and ATF6 (activating transcription factor 6) and IRE1 pathways are anti-apoptotic.

Upon investigation of the UPR pathways in TK strain-induced tumors (which are latently infected with the TK virus) we found a significant transcriptional induction of the ATF6 pathway target, GRP94 (glucose regulatory protein 94). Although not significant, there was an increased transcriptional induction of ATF6 and IRE1 pathway targets, GRP78 (glucose regulatory protein 78) and XBP1(s) (spliced X-box binding protein 1) respectively, while we observed no induction of the PERK pathway target, ATF4 (activating transcription factor 4). Overall, anti-apoptotic mechanisms appear to be induced in the TK-induced tumors. Anti-apoptotic mechanisms mediated by cellular bZIP transactivators, ATF6 and XBP1(s) could be independent of Meq, as bZIP domains of human ATF6 and XBP1(s) were found not to interact with Meq bZIP domain either on a coiled coil array surface or in solution (130). Based on the induction of these targets, MD lymphomas can serve as an excellent model for the targeting of ATF6 and IRE1-XBP1 pathways in order to specifically ablate tumor cells.

While previous studies that analyzed cytokine gene expression (at transcriptomic or proteomic level) in transformed lymphomas have compared sorted CD30^{hi} (transformed) and CD30^{lo} cells populations, we profiled the cytokines at the transcriptional level in the TK induced lymphomas by comparing frank lymphomatous masses to surrounding visibly normal and putatively non-transformed tissue in

affected spleens. This approach would define responses in lymphoma tissue environment that contributes to tumor initiation and progression. We found a significant transcriptional induction of cytokines in lymphomas belonging to the following cell signatures, T_{H1} (IFN- γ , IL-2, T-bet), T_{H2} (IL-4), T_{H17} (IL-17, IL-21, IL-6, TGF- β) and T_{REG} immunophenotypes (IL-4, IL-6, IL-10, TGF- β , IL-2).

INTRODUCTION

1.1 Marek's Disease

Marek's Disease (MD) is a T cell lymphoproliferative and neuropathic disease caused by Marek's disease virus (MDV1). Marek's disease was originally described as a "*generalized polyneuritis*" by a Hungarian veterinarian, Jozsef Marek, in 1907 (101). It was for this seminal work that the disease was named in his honor as Marek's disease in 1960. Since its discovery, the clinical picture of MD has gradually changed over time with the virus tending towards greater virulence.

During the late 1920's, Pappenheimer and his colleagues identified lymphomas in six out of sixty field cases of paralysis examined and described it as "*neurolymphomatosis gallinarum*" based on the similarity between the composition of visceral lymphomas and lymphoid infiltrates in the nervous tissue (120). Although MD was described over the subsequent years, a discernable increase in the virulence of MDV1 field strains was observed twice due to the shift towards high-density poultry production and the near ubiquitous use of vaccination. In the past 25 years, MDV1 strains have continued to evolve towards higher virulence with a concomitant change in the clinical presentation. Along with the pre-existing neurologic and rapid lymphoproliferative lesions, severe brain edema and acute deaths were observed even in vaccinated chickens.

In general, MD is associated with inflammation, profound immunosuppression, lymphoproliferative lesions and neurologic disorders. Common clinical signs of MD include paralysis, skin leucosis, dermatitis, cachexia, visceral lymphomas and neurological signs such as ataxia and torticollis. Losses caused by MD are due to carcass condemnation, secondary infections caused by MD induced

immunosuppression, and MD outbreaks caused by the evolution of field viruses towards higher virulence.

1.2 Marek's Disease Virus (MDV1):

MDV1 was initially classified as a gammaherpesvirus based on its slow growth *in vitro* and its ability to replicate and cause lymphomas in T cells *in vivo*. Based on its structure and the similarity of its genome with other alphaherpesviruses, such as herpes simplex virus (HSV) and varicella zoster virus (VZV), however, it was reclassified as an alphaherpesvirus. Despite this, MDV1 possesses characteristics of both alpha- and gammaherpesviruses with respect to genomic similarity and its ability to replicate, establish latency and transform lymphocytes. MDV1 is a highly cell-associated virus and only infects avian cells explanted *in vitro*.

1.3 Three Serotypes of MDV

MDV isolates were classified into three distinct serotypes all belonging to genus *Mardivirus* (for *Marek's disease-like viruses*). *Gallid herpesvirus 2* (GaHV-2), MDV1, or *Mardivirus 1* includes all the oncogenic strains and their attenuated derivatives. *Gallid herpesvirus 3* (GaHV-3), MDV2, or *Mardivirus 2*, includes all non-oncogenic strains that naturally infect chickens. *Meleagrid herpesvirus-1*, previously serotype 3 MDV, or herpesvirus of turkeys (HVT) includes apathogenic strains that naturally infect turkeys. The sequence of all three genomes has been determined and their similarity ranges between 50-80% at the level of common viral structural glycoproteins, capsid proteins, and enzymes such as DNA polymerase. The genomes of all three viruses are composed of unique long and unique short regions flanked by inverted repeats, known as terminal and internal repeats (long and short).

The overall genomic organization and the linear arrangement of individual genes is similar among all three serotypes and collinear with other alphaherpesviruses such as HSV1 and VZV, whereas the genus or virus specific genes are located primarily in the inverted repeat regions flanking the unique long regions. However considerable variations exist among the three serotypes with respect to virus-specific genes, GC content, and genome size. Genes unique to the MDV1 repeat regions include vTR, vIL-8, RLORF4, 23 kDa protein, *meq*, pp14, and numerous ORFs of unknown function. The genome of HVT encodes a unique 162 aa Bcl-2 homologue in the repeat short regions with anti-apoptotic properties similar to the quail NR-13 protein (69).

The GC content of MDV1 genome (44.1%) is considerably lower than that of MDV2 (53.6%) whereas the GC content of HVT (47.2%) falls in between. Based on the sequence homology and comparison, serotypes MDV2 (SB-1) and HVT (FC-126) elicit vaccinal immunity against MDV1 via their expression of common epitopes from shared antigens, specifically viral structural glycoproteins.

1.4 MDV Pathogenesis:

According to the Cornell model, the pathogenesis of MDV is divided into four phases (26): 1) Early cytolitic phase 2) Latent phase 3) Secondary cytolitic phase, and 4) Transformation. The exact timing and severity of these phases vary depending upon the strain used to infect the chickens, the dose, host genotype, and the age at which they are exposed.

1.4.1 Early Cytolytic Phase:

Keratin-encased, cell-free, and cell-associated MDV are shed along with desquamated feather follicular epithelium from infected birds (10). MDV in dander is stable and can remain infectious for months or perhaps years in the poultry house environment, acting as a source of infection. Initial infection occurs via inhalation into the lung (10). Upon inhalation, the virus is phagocytized by lung epithelium followed by the uptake of virus by recruited macrophages and B cells either directly or after an initial round of replication in lung epithelium (10). Infected B cells and macrophages transmit the virus to bursa, thymus and spleen where virus encounters its major target cell for productive-restrictive lytic replication, the B cell.

In each lymphoid organ, the majority of cytolytically infected cells are B cells but some activated CD4+ T cells are also infected via antigen presenting interactions and undergo apoptosis (107-109). This lymphoid depletion and atrophy occurs in the primary lymphoid organs (bursa and thymus) causing an early immunosuppression. The spleen then becomes a major site of viral replication. Recently established *in vitro* model describing MDV1 pathogenesis identified an efficient infection of CD4+ α ν β ν -TCR2 cells while γ δ TCR1 cells are poorly infected (138). Rapid cytolytic infection occurs and viremia levels peak at 3-7 dpi in chickens with fully functional immune system infected at 3 weeks of age, whereas in the infected day-old chicks, viremia levels peak 7 days later, at 10-14 days post infection.

The genome of MDV encodes a cellular homolog of IL-8, a CXC chemokine known as viral IL-8 (vIL-8) (90). vIL-8 possess a DKR motif instead of heterophil-recruiting ELR motif, and has been shown to recruit PBMCs (122), B cells and CD4+CD25+ T cells (37). vIL-8 plays a major role in MD pathogenesis at various

stages post-infection, promoting lytic replication via recruitment of target B cells resulting in efficient transformation of activated CD4⁺ T cells.

Early MDV lytic replication induces an innate immune response, ostensibly due to vIL-8-mediated recruitment of macrophages during lytic replication and subsequent pro-inflammatory cytokine and interferon production. This drives the virus to undergo latency in activated CD4⁺ TCR2 and TCR3 cells infected through direct antigen presenting interactions with antigen presenting cells (B cells, macrophages and dendritic cells). This innate immune response is characterized by the production of NO and pro-inflammatory cytokines such as IL-1 α/β , IL-6, IL-8, as well as Type I and II interferons (32, 62, 66). By 7-10 days post-infection, lytic gene expression is completely repressed, although the viral genome persists in infected cells marking the shift from cytolytic phase to latency.

1.4.2 Latent Phase:

The latent phase is defined as presence and maintenance of viral genomes without any virus particles being formed. During latency, viral genome integration into the host telomeres occurs via TMR arrays located in *a-like* sequences at the viral genome termini. High integration efficiency is necessary, although not sufficient for efficient tumor formation and subsequent reactivation (48, 67). MDV undergoes latency primarily in the activated CD4⁺ TCR2⁺ and TCR3⁺ T cells, although some reports have shown latent MDV in B cells, CD4⁻CD8⁻ T cells and CD4⁻CD8⁺ T cells (119, 137). Latently-infected CD4⁺ T cells rapidly proliferate and disseminate the virus to various visceral and peripheral sites by blood.

1.4.3 Secondary Cytolytic Phase:

As the innate immune response maintaining the latency wanes, the virus reactivates and a second wave of cytolytic infection ensues at the peripheral sites (e.g. adrenal glands, kidneys, Schwann cells and feather follicular epithelium). Fully productive virus replication occurs only in the feather follicular epithelium with the cell-free and cell-associated virus being shed intermittently throughout the life of chicken even in vaccinated and protected chickens. The MDV genome load in the feather follicles was found to correlate with the genetic background of the chicken, with the MDV genome load being significantly lower in MDV resistant birds compared to MDV susceptible birds at 21 dpi (6). In addition, an increase in pro-inflammatory cytokine expression levels was observed in the feather pulp along with CD4+ and CD8+ CTL infiltration (4).

1.4.4 Phase of Transformation:

During latency, some of the latently-infected CD4+ T cells will proliferate and give rise to lymphomas. MDV infection can result in tumor formation in multiple visceral organs including the heart, kidneys, spleen, gonads, intestines and proventriculus. The efficiency of MDV-mediated transformation depends upon the robustness of primary lytic replication being able to generate sufficient number of latently infected CD4+ T cells necessary for transformation. Latency is a necessary event although insufficient for transformation to occur. During the phase of transformation, transformed T cells begin to appear with visceral lymphomas formed by 4-6 weeks post-infection depending upon virus strain, host genetic susceptibility, and environmental factors.

Target cells for natural MDV-mediated transformation are primarily CD4+ CD8- T helper cells. The phenotype of MDV transformed CD4+ T helper cell was established based on studies done in lymphoblastoid cell lines derived from MDV induced lymphomas. The cell lines derived from naturally occurring lymphomas had mainly CD4+ T cells with either TCR2+ or TCR3+. Whereas, the cell lines derived from local MDV induced lesions were composed of 21% CD4+ CD8- cells and the remaining were CD4- CD8+. Double negative CD4- CD8- and CD8+ T cells were also found to be transformed, although they are very less permissive to transformation.

The transformed component of MD lymphomas are CD30^{hi} (22) with an overall cytokine profile depicting T_{REG}-like immunophenotype (145). CD4+ T cells undergoing transformation depict distinctive changes in their surface antigen expression along with viral genome integration at multiple sites in a random manner (121). MDV tumors are monoclonal or oligoclonal in nature with the transformed CD4+ T cells skewed towards having T regulatory like immune phenotype (114). A permanent phase of immune suppression ensues in response to transformed T_{REG}-like immunophenotype of lymphomas.

1.4.4.1 The *meq* Oncogene

Among the MDV gene products directly linked to transformation, Meq (Marek's EcoRI-Q-encoded protein) encoded in the repeat regions (TR_L and IR_L) flanking the unique long (U_L) sequences was found to be consistently expressed in virus-induced tumors and tumor-derived lymphoblastoid cell lines (65). Genetic comparison among MDV1 strains with distinct virulence levels have led to the identification of characteristic mutations in the coding sequence of Meq that correlate with virulence (146). As these mutations have also been identified in the chickens

vaccinated with HVT and SB1, vaccine viruses lacking *meq* gene, it was suggested that the mutations in *meq* arose in response to functional selection on MDV-host cell interactions rather than immune selection against common surface glycoproteins (146).

Mild and virulent MDVs (m/vMDVs) isolated during the 1960s and 1970s tend to encode a larger form of Meq (398 aa) composed of five or more proline rich repeats (PRRs) in their C terminus, whereas very virulent and very virulent plus MDVs (vv/vv+MDVs) encode a smaller length Meq (339 aa) with three PRRs.

In the US, vv+MDVs also have mutations at the second position of polyproline tracts (PPPP → P(Q/A)PP) (146). Higher number of PRRs is associated with lower transcriptional activation potential. On the other hand, point mutations in the PRRs in Meqs of higher virulence were found to have enhanced transactivation or transformation potential.

A P217A mutation introduced in RB1B Meq that corresponds to MD5 Meq at the second position of PRR enhances transactivation potential of Meq and vice versa (111). Similarly, mutations in basic region 2, a region encoding nuclear and nucleolar localization signals (NLS, NoLS), in addition to DNA-binding, were also found to alter transcriptional activity (112). Inhibiting the expression of Meq with either siRNAs or antisense oligos reduced growth and soft agar colony formation in the transformed DF1 and MSB1 cell lines, respectively (82, 170).

Overexpression of Meq in rat fibroblast cell line (Rat-2) lead to enhanced proliferation and apoptosis resistance in addition to serum and anchorage independent growth (91). Deletion of *meq* or a single mutation in its CtBP-interaction domain (pro-leu-asp-leu-ser, PLDLS) fully attenuated the virus in its ability to cause tumors *in vivo*

(17, 94). The full-length, unspliced Meq protein is expressed throughout the course of infection and has been shown to rapidly localize into the nucleoplasm, nucleoli and Cajal bodies whereas the splice variants of Meq are expressed during latency and tend to possess low mobility (9).

Meq homodimerizes with itself or heterodimerizes with cellular bZIP proteins such as c-Jun, ATF-1, -2, -3 CREB and Fra-2 (82). Using a coiled-coil array, bZIP domain of Meq was shown to interact with additional cellular bZIP proteins ATF-2, Jun-B, Jun-D, DDIT3 and NFIL3 in solution (130). Meq was found to form stable dimers with c-Jun potentiating the downstream signaling leading to upregulation of v-Jun targets Hb-EGF, JTAP-1 and JAC (82). Other known interacting partners of Meq include cell cycle regulatory proteins CDK-2, p53, and Rb (76), CtBP, a protein involved in forming transcriptional repression complexes (17), and HSP70, a molecular chaperone involved in neoplastic transformation (180).

Meq interacts with CtBP dimers via a PLDLS domain in its N-terminus and functions to repress select genetic loci, possibly both viral and cellular, by recruiting transcriptional repression complexes composed of chromatin modifying enzymes (HMTs, HDACs, HATs) (17). Depending on its dimerization partner, Meq targets distinct promoters, causing either transcriptional activation or repression (82). Based on its ability to regulate massive lytic replication and associated pro-inflammatory responses, along with enhanced proliferative and anti-apoptotic properties, Meq serves as an important switch between lytic and latent phases of infection. This is evident from the basis of protection against vv+ challenge conferred by two highly protective vaccines, RM1 and rMD5ΔMeq, derived upon attenuation of virulent JM102/W by insertion of REV LTR into its genome (64) and deletion of both copies of *meq* from

the vvMDV, rMd5 (94) respectively. Both the vaccines induce severe thymic atrophy in maternal antibody-negative (Mab-) chickens causing target CD4+ T cell loss.

Chapter 2

EVALUATION AND VALIDATION OF REFERENCE GENE STABILITY DURING MAREK'S DISEASE VIRUS INFECTION

2.1 Introduction

Real time PCR has been a widely used tool for accurate quantification of both DNA and RNA in the field of virology (98). Many factors such as methodology employed for the extraction of RNA, quality and quantity of RNA, presence of inherent inhibitors, efficiency of reverse transcription and PCR amplification affect the sensitivity of the qRT-PCR (25). In addition, poor assay design or experimental conditions and inappropriate normalization strategies compromise the integrity of the resulting data (24). Various methods of normalization have been proposed such as normalization to sample size (cell number), total RNA or genomic DNA, and the use of standard reference genes have been used for normalization of expression (58, 155).

Normalization to cell number is not possible if the experimental sample is a whole tissue. Normalization to total RNA or genomic DNA can be affected by variation in the extraction rates with the final yields being quite low in either quality or quantity. In addition, normalization to total RNA/DNA do not take into account the variation in the efficiency of reverse transcription or qRT-PCR amplification (150). Normalization to total DNA poses an additional draw back in the presence of multiple haplotypes in tumor cells (58, 155), or the presence of multiple copies of particular loci in replicating bacteria in comparison to non-replicating bacteria (133).

Normalization to internal control reference genes has been the most popular and reliable method of normalization due to the fact that it considers and precludes the

error due to initial RNA/cDNA loading and also the variation in the efficiency of reverse transcription and qRT-PCR reaction (58). Normalization to the geometric mean of multiple reference genes has also been suggested as an accurate way of normalization, although it is not possible to use multiple reference genes all the time due to limitations in sample availability, increased expense, and variability in one of the selected reference genes challenging the accuracy. However, it is the most rigorous and conventional method of normalization.

The concept of using reference genes for normalization is based on the assumption that the expression of reference genes remains the same under any experimental condition, although this may not be the case in a real life scenario. Hence, any fluctuations in the expression of reference genes selected as internal controls produce erroneous interpretation of biological results (161).

Based on the published literature, expression of different reference genes varies among different tissues under different experimental conditions, at various developmental stages, and also during disease (35). Therefore, identification and validation of ideal reference genes with constant or stable expression levels under various experimental conditions is important to produce biologically-relevant data (139).

Real time PCR has been widely used in many studies to define cellular responses to MDV infection or vaccination, and also to elucidate mechanisms of MD pathogenesis and tumor development (1, 3-6, 41, 66, 86, 106). Additionally, it is also being used for the absolute quantification of viral loads or viremia levels and for correlating these to various factors associated with the outcome of disease such as host

genotype, immune or viral gene expression, and viral shedding via feather follicular epithelium (2, 11, 45, 60).

Chicken embryo fibroblast (CEF) cultures or fibroblast derived cell lines (DF1, OU-2, SOgE) are mainly used for the propagation of MDV *in vitro* and to study the functionality of MDV-encoded genes and gene mutations. Given the highly cell-associated nature of MDV, infection with MDV is associated with global expression changes in both mRNA and ribosomal RNA levels (106). Target gene normalization based on varying housekeeping gene can therefore produce misleading results. Hence, it is important to validate the stability of housekeeping gene to ensure that the selected reference gene is unaffected under MDV infection both *in vitro* and *in vivo*.

In the current study, we have evaluated the stability and suitability of five of the most commonly-used reference genes (β -actin, 28S RNA, 18S RNA, GAPDH and PPIB) as standard internal controls *in vitro* in CEF cultures infected with four pathotypes of oncogenic MDVs and three vaccine strains. Additionally, we have also evaluated the stability of the above mentioned five reference genes *in vivo* in vv+ MDV1 (TK, or T King)-induced spleen tumors.

The candidate reference gene stability was evaluated using two excel based algorithms Bestkeeper and Normfinder (8, 150). Separate analyses were carried out for oncogenic and vaccine strains *in vitro* and TK induced spleen tumors *in vivo*. The results obtained from Bestkeeper and Normfinder were confirmed by another web based tool known as Reffinder (<http://www.leonxie.com/referencegene.php>). Bestkeeper determines the stability by calculating the standard deviation and coefficient of variance from the input Ct values and the reference gene with lowest standard deviation is considered most stably expressed. Reference genes with standard

deviation [SD (\pm Ct)] greater than 1 are considered least stable. In addition, the geometric mean of Ct values for each of the reference gene in a given sample is combined in a Bestkeeper Index (BI). Bestkeeper then performs a pairwise correlation analyses between each reference gene and assigns a Pearson correlation coefficient (r value) and probability value (p value) for each gene combination in order to determine the relationship between them. Highly correlated genes are combined into an index (BI) and the correlation between each gene pair and BI is calculated as correlation coefficient (r value). The genes with significantly higher correlation coefficients (r value) are considered the most stable reference genes. The average Ct values of technical duplicates were imported into Bestkeeper (version 1) to calculate the stability.

Normfinder calculates intergroup (between the groups) and intragroup variations (within the groups) and then combines both of them to calculate the stability value for each gene. Since the stability value is a combination of two sources of variation, it represents a practical measure of systematic error introduced by a gene when used as a housekeeping gene. The gene with lowest stability value (M number) is considered the most stably-expressed reference gene. For each reference gene of interest, the Ct values were converted into relative quantities of the lowest Ct value, which is set to 1. The log-transformed data is then analyzed using Normfinder to calculate the stability values. The Bestkeeper algorithm is resistant to sampling errors, while it is a requisite that none of the selected genes for Bestkeeper analysis are co-regulated. Normfinder is less sensitive to co-regulated genes while it is highly sensitive to sampling errors. Hence the use of a combination of both Bestkeeper and Normfinder provides a more robust analysis in evaluating the stability of candidate

reference genes. Reffinder is a web tool that combines geNorm, Normfinder, BestKeeper and comparative Δ Ct methods to compare and rank each reference gene.

2.2 Materials and Methods

2.2.1 Cells and Viruses:

For the propagation of MDV1 serotypes and vaccine strains, secondary chicken embryo fibroblasts (CEF) were prepared from 10-day-old specific pathogen free (SPF) embryos (Sunrise Farms, Inc. Catskill, NY). Secondary CEF were propagated in M199 medium supplemented with 3% filtered calf serum, L-Glutamine and antibiotics (all reagents from Gibco, Carlsbad, CA) and maintained at 37°C in 5% CO₂ humidified chamber. CEF were infected in triplicates with 5000 PFU of each strain and harvested upon the appearance of plaques on Day 5. All the oncogenic viruses, CU2 (a mildly virulent MDV, obtained originally from Dr. K.A. Schat, Cornell University), RB-1B (a vvMDV, originally obtained from Dr. K.A. Schat), rMd5 (originally obtained from Dr. Sanjay Reddy, Texas A & M University), and T KING (TK, a vv+MDV, originally obtained from Dr. John K. Rosenberger, University of Delaware) and vaccine strains (HVT, SB-1, and CVI-988, all obtained from Merial, Inc., Gainesville, GA) described in the study were from the stocks of Parcels' laboratory.

2.2.2 *In vivo* Tumor Collection:

Solid tumor masses were isolated from unvaccinated commercial broiler chickens (Hubbard X Cobb) infected via contact with the vv+MDV (TKING) strain of MDV1 during a vaccine efficacy study. Tumors were obtained at necropsy performed at the end of the seventh week post hatch. Frank lymphomas were obtained from

spleens (n=4), and were excised from the surrounding non-tumorous spleen tissue. In addition, as an infected control, phenotypically non-tumorous adjacent counter parts (n=4) were collected from the corresponding tumorous spleens. To serve as negative controls, healthy normal spleens (n=4) from uninfected and unvaccinated chickens housed separately were also collected. Spleen samples were collected into RNA later (Ambion Inc., Austin, TX) and stored at -80°C for further RNA purification.

2.2.3 Quantitative RT-PCR Analysis:

Total RNA was isolated from harvested cells/spleen tissues using Qiagen RNA/DNA/Protein Kit according to the manufacturer's instructions (Qiagen, USA). Total RNA quality (260/280 ratio) and quantity (at 260 nm absorbance) were measured using an Agilent Nanodrop spectrophotometer. 1µg of total RNA was reverse transcribed with random hexamers using the High Capacity cDNA Reverse Transcription Kit (Applied Biosystems, USA), as recommended by the manufacturer's protocol (Step 1: 25°C for 10 min; Step 2: 37°C for 120 min; Step 3: 85°C for 5 min; Step 4: 4°C until samples are removed).

The final cDNA was diluted 10 fold and 1µl of final cDNA dilution was used in a 20 µl reaction consisting of 10 µl iQTM SYBR® Green Supermix (Bio-Rad, Hercules, CA), 8.2µl of nuclease free water and 250nM each of forward and reverse primers. Quantitative real time PCR was performed using SYBR green chemistry as recommended by the manufacturer (Bio-rad Laboratories) on the MyiQ2 Two Color Real Time PCR Detection System (Bio-rad Laboratories, Hercules, CA). Following amplification and collection of raw fluorescence data, melt curve analysis was performed to exclude the possibility of non-specific amplification.

2.2.4 Primer Design:

Primer sequences for the reference genes β -actin, 28S RNA, 18S RNA, GAPDH and PPIB are provided in Appendix A.

2.3 Results

According to Bestkeeper analysis (Table 2.1), β -actin was determined to be the least stable reference gene with a higher standard deviation [SD (\pm Ct)] under *in vitro* infections with either oncogenic strains [\pm 0.85] (Figure 2.1) or vaccine strains [\pm 0.83] (Figure 2.2) and also in RNA from *in vivo* TK-induced spleen tumors [\pm 1.2] (Figure 2.3). Although the standard deviation is not greater than 1, β -actin has the highest standard deviation among the validated reference genes in *in vitro* experimental infections with either oncogenic or vaccine serotypes.

Among the most stable reference genes, 28S RNA displayed the highest stability with lowest standard deviation in oncogenic strains treatment [\pm 0.3] and TK-induced spleen tumors [\pm 0.62] while PPIB displayed the highest stability in vaccine strain treatment [\pm 0.35].

In general, 28S RNA and PPIB displayed the highest stability among oncogenic strain treatment [$0.3 < SD < 0.37$] and vaccine strain treatment [$0.35 < SD < 0.39$]. In TK-induced spleen tumors, PPIB (SD \pm 0.72) ranked second after 28S RNA (SD \pm 0.62).

With respect to correlation coefficients between Bestkeeper index and the studied reference genes, there was some amount of inconsistency (Table 2.2). This is because the use of Bestkeeper's correlation coefficients and the corresponding *p* values are limited to groups without heterogeneous variance between gene expression levels. However, in our case, there was a difference in the expression levels (Ct

values) of selected reference genes contributing to significant variances. Ct values in our study varied from ~13 (28S RNA), ~16 (18S RNA), ~ 22 (β -actin) to ~25 (GAPDH and PPIB). In general, the most stably expressed reference gene according to Bestkeeper, 28S RNA, displayed significantly higher correlation with Bestkeeper index.

According to the Normfinder analysis (Figure 2.4), 28S RNA and PPIB were considered as the most stably-expressed reference genes with the lowest M values or stability numbers among all the treatments and reference genes under validation. β -actin was determined as the least stable reference gene with highest M value. Altogether, both Bestkeeper and Normfinder determined 28S RNA and PPIB as the most stable reference gene candidates among the five reference genes tested under given experimental conditions, while β -actin proved to be the least stable reference gene.

<i>Treatment</i>	<i>BACT</i>	<i>28S RNA</i>	<i>18S RNA</i>	<i>GAPDH</i>	<i>PPIB</i>
<i>Oncogenic strains (n=15)</i>	0.85	0.30	0.61	0.54	0.37
<i>Vaccine strains (n=12)</i>	0.83	0.39	0.38	0.44	0.35
<i>TK induced tumors (n=12)</i>	1.20	0.62	0.84	0.91	0.72
<i>Overall SD average</i>	0.96	0.44	0.61	0.63	0.48

Table 2.1: Bestkeeper analysis of housekeeping genes showing variation in gene expression. Values are represented as standard deviation (SD \pm Ct). Bestkeeper analysis revealed β -actin to be the most unstable gene among all the treatments tested with an overall high SD average. 28S RNA and PPIB turned out to be the most stably expressed reference genes with an overall average varying between 0.44 and 0.48 respectively.

<i>Bestkeeper coefficient of correlation (HKG vs Bestkeeper index)</i>					
<i>Treatment</i>	<i>BACT</i>	<i>28S RNA</i>	<i>18S RNA</i>	<i>GAPDH</i>	<i>PPIB</i>
<i>Oncogenic strains</i>	0.668 ^A	0.892 ^A	0.812 ^A	0.746 ^A	0.655 ^A
<i>Vaccine strains</i>	0.021	0.727 ^A	0.467 ^A	0.735 ^A	0.249
<i>TK induced tumors</i>	0.945 ^A	0.892 ^A	0.967 ^A	0.859 ^A	0.931 ^A

Table 2.2: Pairwise correlation analyses between reference genes and bestkeeper index. Superscript letter A indicates significance at $p < 0.05$ level.

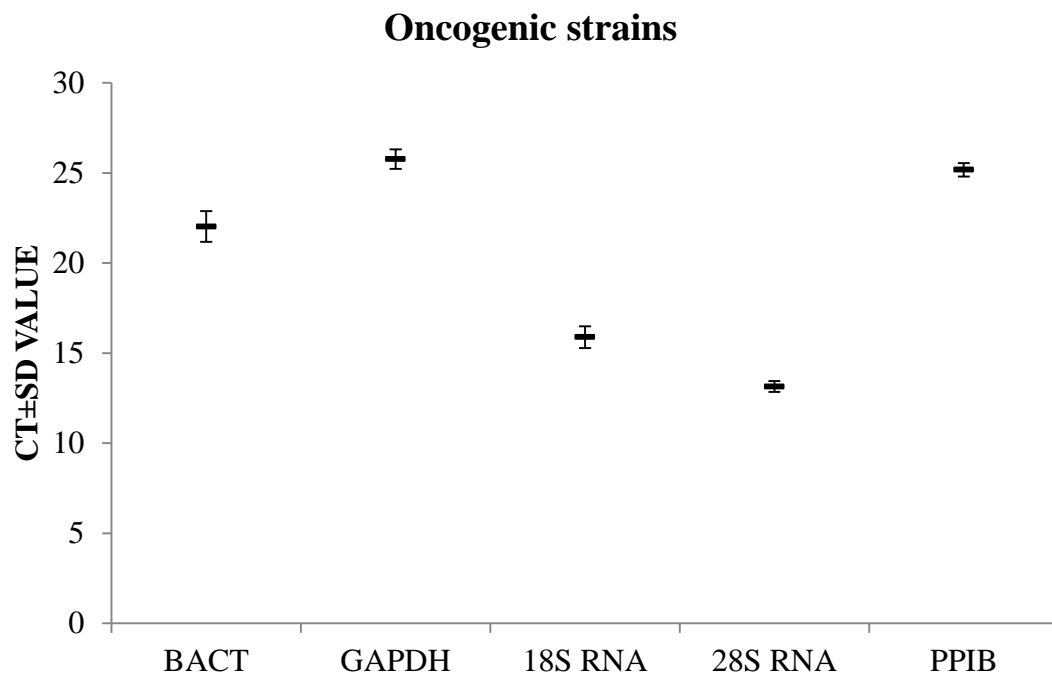


Figure 2.1 Graph representing best keeper analysis of stability in their order of ranking from least stable to most stable. Y-axis represents threshold cycle \pm standard deviation. X-axis represents reference genes included in the analysis.

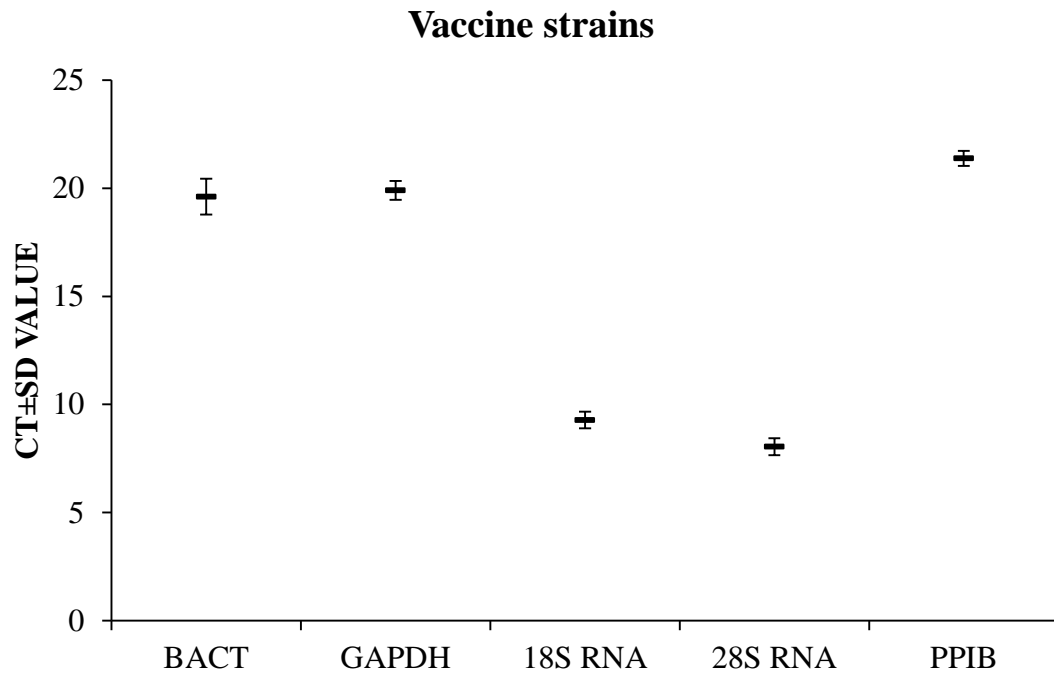


Figure 2.2: Graph representing best keeper analysis of stability in their order of ranking from least stable to most stable. Y-axis represents threshold cycle \pm standard deviation. X-axis represents reference genes included in the analysis.

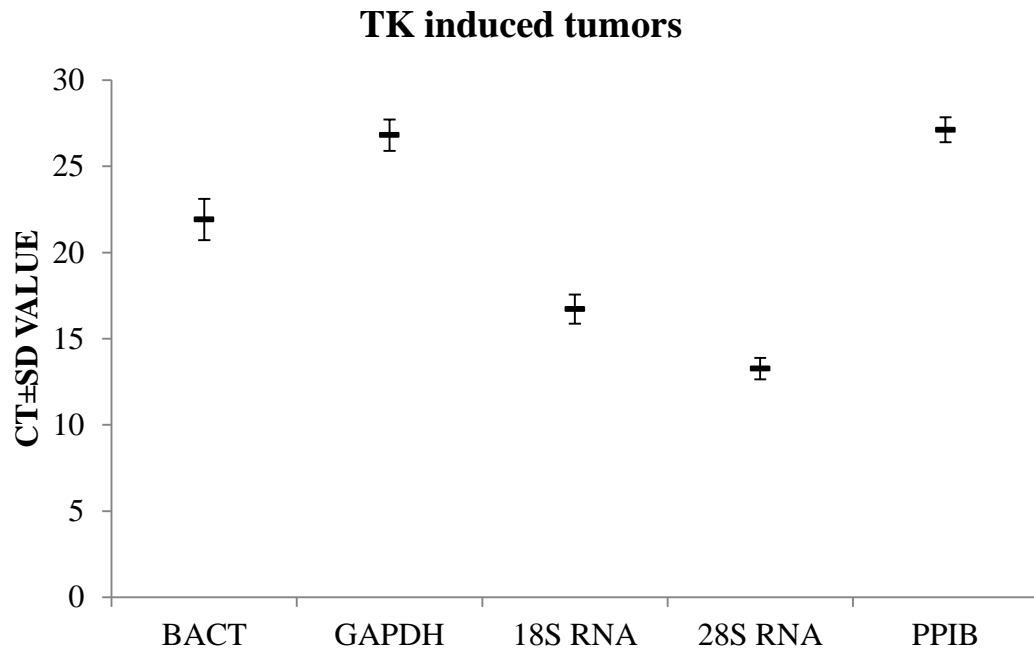


Figure 2.3: Graph representing best keeper analysis of stability in their order of ranking from least stable to most stable. Y-axis represents threshold cycle \pm standard deviation. X-axis represents reference genes included in the analysis.

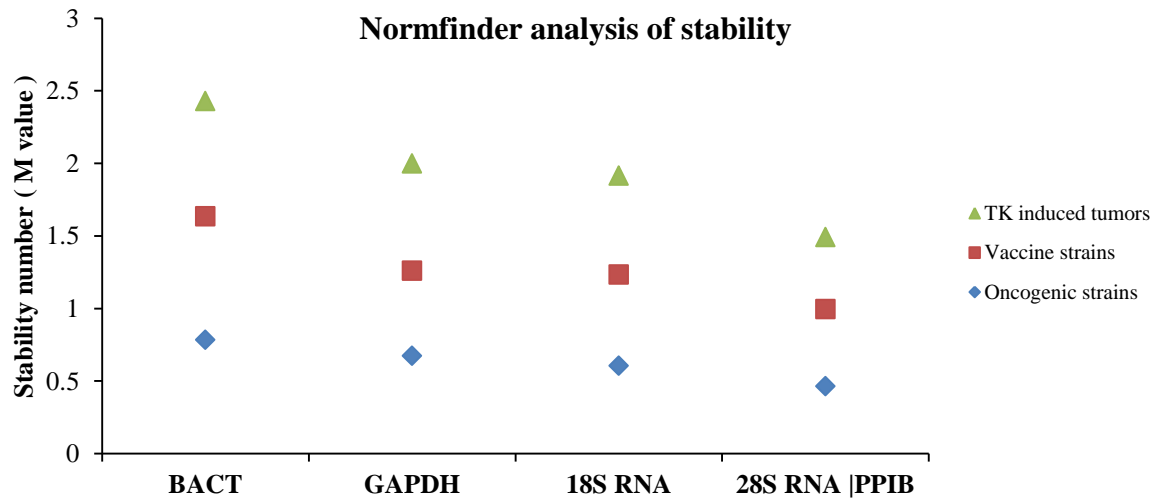


Figure 2.4: Graph representing Normfinder analysis of stability in their order of ranking from least stable to most stable. Y-axis represents stability number or M value. X-axis represents reference genes included in the analysis.

2.4 Discussion

Our data is consistent with previous reports where β -actin was shown as a least stable reference gene in the context of herpesviral infections (127, 168). Actin was known to play an important role during herpesvirus infection of cells, from viral entry until egress. HSV1 glycoprotein binding to host cell surface receptors and entry into the cells via fusion was found to rely on cortical actin.

In order to mediate actin dependent entry and infection upon receptor binding, HSV1 was found to stimulate Rho GTPase signaling (Rho1, CDC42, Rac1) altering the morphology of cortical actin. Also, intranuclear movement of nucleocapsids towards the inner nuclear membrane was found to be ATP dependent and sensitive to actin depolymerizing agent latrunculin A but not cytochalasin D (38). Herpesvirus nucleocapsids were thought to induce nuclear actin polymerization to promote their movement towards inner nuclear membrane for primary envelopment via myosin motors. Among the HSV1 proteins involved in primary envelopment at the inner nuclear membrane and subsequent de-envelopment at the outer nuclear membrane respectively, are U_L11, U_L31, U_L34, U_L53 (gK), and U_S3.

Deletion of US3 in HSV1, PRV and MDV1 resulted in an accumulation of nucleocapsids between the two leaflets of nuclear membrane with a subsequent reduction in viral titers (70, 126, 131, 134, 142, 143). The US3 kinase has been shown to be a crucial player in the de-envelopment of primarily enveloped virions by fusing with the outer leaflet of the nuclear membrane resulting in naked nucleocapsids in the

cytoplasm. US3 also appears to possess anti-apoptotic function and an ability to mediate actin stress fiber break down.

Upon MDV1 infection of chicken embryo cells, US3 null mutants have reduced plaque titers with an increase in accumulation of enveloped virions at the perinuclear space and a corresponding decrease in number of viral particles in cytoplasm. US3 kinase was demonstrated to mediate cytoskeletal rearrangement during earlier phases via transient actin stress fiber break down with a subsequent regeneration, possibly due to the cellular stress response (143). Furthermore, inhibiting actin repolymerization or causing actin depolymerization, but not microtubule depolymerization, was shown to inhibit cell-to-cell spread of MDV, *in vitro*. However, in a later study, it has been demonstrated that growth defects observed with the US3 null mutant is due to a lack of kinase activity towards its target substrate, pp38, rather than F-actin disassembly (142).

Another study has demonstrated a key role played by Rho-ROCK signaling and actinomyosin in facilitating cell-to-cell spread of MDV, while Rac-PAK signaling had an opposing effect (132). Given the diverse ways of cellular actin exploitation by herpesviruses in order to promote infection and spread, it is not uncommon that actin is the most deregulated gene at transcriptional level during infection by herpesviruses.

While one study by Watson *et al.*, noted PPIA, GAPDH and SDHA as stable reference genes in their decreasing order of stability in HSV, CMV and VZV infected cells, another study by Radonic *et al.*, noted TBP and PPIA as the most stably-expressed reference genes under infections with CMV, HHV-6, CAMP, SARS and YF viruses.

In our study, we did not include PPIA. However, we did include a closely related cyclophilin family member, PPIB, which was found to be equally stable along with 28S RNA in the context of MDV infection. Finally, 28S RNA and PPIB were found to be most stably expressed reference genes, while β -actin proved to be the least stable reference gene, with GAPDH and 18S RNA being only slightly more stable during MDV1 infection or in tumor cells. Due to lack of a poly-A tail, 28S RNA cannot be employed as a reference gene when reverse transcription priming is via oligo-dT. PPIB can serve as a reference gene when the reverse transcription priming is by either random oligos or oligo dT.

Chapter 3

INDUCTION OF THE UNFOLDED PROTEIN RESPONSE (UPR) DURING MAREK'S DISEASE VIRUS (MDV) INFECTION

3.1 Endoplasmic Reticulum:

The endoplasmic reticulum (ER) is a major cell organelle that plays an important role in the biosynthesis of proteins and lipids. The ER is composed of a network of interconnected branching tubules and flattened sacs extending from the cell membrane throughout the cytoplasm to the nuclear membrane. The ER is the principle site for biosynthesis, folding, assembly, modification and maturation into biologically-active proteins. The ER exists in two forms in the cell, rough ER (rER) with ribosomes studded on the outer surface, and smooth ER (sER) with no ribosomes on the surface.

Newly synthesized polypeptides in the cytoplasm are transported to ER where they undergo various post-translational modifications before being translocated and embedded either in cellular membranes or secreted out of the cell. These proteins are either transmembrane proteins, which are partly translocated and embedded in the ER membrane, or water-soluble proteins, which are completely translocated across the membrane into the ER lumen.

In the ER, these proteins are folded into their native three-dimensional structures with the aid of molecular chaperones and undergo various post-translational modifications, such as the addition or modification of carbohydrate moieties. Upon modification in the ER, proteins are transported to either the appropriate cellular compartment or golgi apparatus for further modification.

The smooth ER is mainly involved in the synthesis of lipids or lipoproteins, maintenance of Ca^{2+} homeostasis, and detoxification or metabolism of drugs and chemicals. The smooth ER is also involved in the transport of newly synthesized proteins from rough ER to golgi apparatus.

Folding and modification of proteins is a post-translational process necessary for the proteins to attain their native three-dimensional structure, an essential step in carrying out their function (51, 68, 100). The ER maintains an inherent and highly efficient quality control system ensuring proper folding of proteins. This quality control system senses and retains any unfolded, mis-folded, or unassembled proteins in the ER and targets them for degradation through the ER-associated degradation process (ERAD). By this process, any defective proteins are prevented from reaching their target compartments (59). This quality control system of ER is composed of chaperones, protein folding enzymes and signal transduction pathways necessary for maintaining the proper function of the ER.

3.2 ER Stress and The Unfolded Protein Response (UPR):

Any dysfunction of the ER is known as ER stress. ER stress can result from a variety of factors such as hypoxia, glucose deprivation, over nutrition, Ca^{2+} depletion or disruption of Ca^{2+} homeostasis, bacterial or viral infections, accumulation of unfolded or misfolded proteins due to excessive protein influx, cold or heat stress, and pharmacological agents affecting protein glycosylation (e.g. tunicamycin), Ca^{2+} balance (e.g. thapsigargin), and ER-Golgi vesicular transport (e.g. Brefeldin A).

Approximately one third of newly-synthesized proteins are targeted for proteasome-mediated degradation due to defects in their protein folding (141). Any increase in the translation or influx of secretory proteins into the ER can cause an

accumulation of mis-folded proteins. This transient increase, complemented with other perturbations in ER function, such as alterations in the redox status, Ca²⁺-balance, or improper post-translational modifications would amplify the ER stress (77). To cope with the adverse effects of ER stress due to mis-folded proteins, the cell activates an adaptive response known as unfolded protein response (UPR).

The unfolded protein response is an evolutionarily-conserved mechanism by which cells sense and respond to the accumulation of mis-folded or unfolded proteins in the ER. The UPR is triggered via three type I transmembrane stress sensors located in the ER: inositol 3-requiring enzyme1 (IRE1), protein kinase R (PKR)-like ER kinase (PERK), and activation transcription factor 6 (ATF6) (42, 68, 97).

Under normal physiological conditions, UPR signaling sensors residing in the ER membrane are suppressed, or held in check via the binding of immunoglobulin heavy chain binding protein/glucose regulatory protein 78kDa called BiP/GRP78 (42, 68, 97). Upon ER stress due to the accumulation of improperly-folded proteins, BiP is released from three primary transmembrane signaling sensors IRE1, PERK, and ATF6, resulting in their activation leading to downstream signaling to the nucleus. This activation was thought to be mediated by multiple mechanisms, including competitive-binding of BiP by misfolded proteins, direct sensing of misfolded proteins by the luminal domains of PERK and IRE1 and active dissociation of BiP from ATF6 through an unknown mechanism.

3.2.1 Inositol-1 Requiring Kinase (IRE1) Signaling:

Upon activation of UPR and release of BiP from the luminal domain, IRE1 oligomerizes allowing trans-autophosphorylation of juxtaposed kinase domains. This leads to activation of IRE1, which now has a dual enzymatic function, as a kinase and

an endoribonuclease. The only known target of the activated IRE1 endoribonuclease is the mRNA encoding the transcription factor XBP1. The endoribonuclease function of activated IRE1 cleaves a 26 bp intron from XBP1 mRNA, resulting in a frameshift and removal of a premature stop codon (Figure: 3.2).

This unconventionally-spliced XBP1(s) encodes a full length active transcription factor with bZIP and C-terminal transactivation domains, while the unspliced form XBP1(u) lacks the transactivation domain and functions as a repressor. XBP1(s) protein translocates into the nucleus and transactivates the genes necessary for protein folding, protein entry into the ER, protein degradation (ERAD), and also lipid biogenesis necessary for the expansion of the ER (51, 53, 68, 140). Activated IRE1 also functions as a non-specific nuclease and promotes degradation of ER membrane-associated protein coding mRNAs in a process known as regulated IRE1-dependent decay (RIDD) (54, 55).

With respect to its kinase activity, IRE1 forms a multi-molecular complex with TNF receptor associated factor 2 (TRAF2) and apoptosis signaling kinase 1 (ASK1) known as “UPRosome” triggering the activation of multiple downstream signaling pathways (JNK, p38 and MAPK) causing an activation of the pro-apoptotic Bcl-2 homology 3 (BH3) and inhibition of anti-apoptotic Bcl-2 (B-cell lymphoma 2), ultimately leading to apoptosis under prolonged unresolved UPR (169).

3.2.2 PERK Signaling

Upon activation of UPR and release of BiP, PERK dimerizes and transautophosphorylates its cytosolic kinase domains. Additionally, the activated PERK dimer phosphorylates the α -subunit of eukaryotic translation initiation factor 2 alpha (eIF2 α) at serine 51, causing translation attenuation in an effort to reduce the ER

client load. Phosphorylated eIF2 α has increased affinity for guanosine diphosphate (GDP) and prevents the exchange of guanosine diphosphate (GDP) for guanosine triphosphate (GTP) in the eIF2 α -GDP complex by inhibiting guanosine exchange factor (GEF) eIF2B and thus eIF2 activation. Since GTP bound eIF2 is necessary for the recruitment of the initiator methionyl-tRNA (tRNA_{Met}) to the 40S ribosome, forming a 43S pre-initiation complex to initiate downstream scanning for an initiator codon and subsequent binding of 60S subunit, the absence of an active eIF2 α -GTP-tRNA_{Met} ternary complex precludes the formation of 80S initiation complex required for translation, and thus, a decrease in the overall translation rate occurs (33, 51).

Phosphorylated eIF2 α , however, promotes the selective translation of ATF4 via the 'uORF bypass scanning mechanism'. ATF4 mRNA encoding a bZIP transcription factor, has two upstream open reading frames (uORF), in its 5' untranslated region. During unstressed conditions, abundant GTP-bound eIF2 allows the ribosomes to scan downstream of uORF1 to reinitiate at the next coding region, uORF2, which has an inhibitory element that blocks ATF4 expression. Under stressed conditions, lower levels of GTP-bound eIF2 delays re-initiation, increasing the time required for the ribosomes to scan through the inhibitory element in uORF2 ultimately bypassing it and reinitiating at the ATF4 coding region (166).

Upon translation, ATF4 translocates to nucleus and transactivates genes involved in the amino acid transport, antioxidant response, and apoptosis regulation such as growth arrest and DNA damage (GADD34), ER oxidoreduction1-like protein (EROL1) and C/EBP homologous protein (CHOP). Once homeostasis is restored in the ER, ATF4-induced GADD34 associates with protein phosphatase 1 to

dephosphorylate eIF2 α and inactivate the PERK pathway in a negative feedback mechanism (53, 68, 140).

Similarly XBP1-induced P58^{IPK} also binds PERK and inhibits its kinase activity in a negative feedback mechanism (78, 165). Under prolonged and unresolved UPR, chronic PERK activation allows increased steady-state levels of shorter half-life proteins, ATF4 and CHOP, to activate apoptotic cell death.

3.2.3 Activating Transcription Factor 6 (ATF6) Signaling:

In normal, unstressed cells, ATF6 is bound by BiP on its luminal domain, preventing its activation. In stressed conditions, BiP dissociates from ATF6, unmasking its Golgi localization signal, enabling its transport from the ER to the Golgi. Upon transit to the Golgi, ATF6 is cleaved by the site-specific proteases S1P and S2P to release the cytosolic portion containing bZIP and transactivation domains (173). Cleaved ATF6 translocates to the nucleus and binds to the ER stress responsive elements (ERSE) in the promoters of target genes coding for ER chaperones such as immunoglobulin heavy chain-binding protein or Glucose Regulatory Protein 78 (BiP/GRP78), Glucose Regulatory Protein 94 (GRP94), calreticulin and components of ERAD resulting in transactivation of target genes (18, 51, 68).

Altogether, these three primary signaling mechanisms converge in enabling cells to cope with the stress by inhibiting translation to reduce ER client load, enhancing protein folding, and targeting mis-folded proteins for ERAD, with prolonged unresolved UPR leading to apoptosis (Figure 3.1).

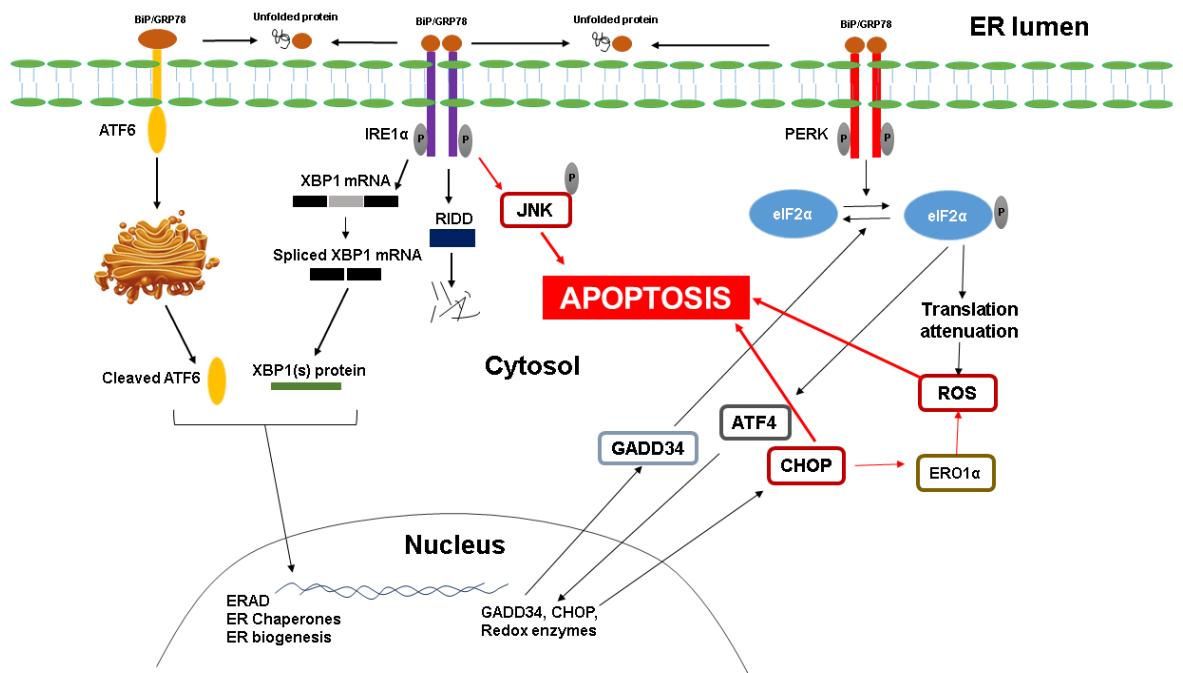


Figure 3.1: Schematic Illustration of UPR Signaling Pathways.

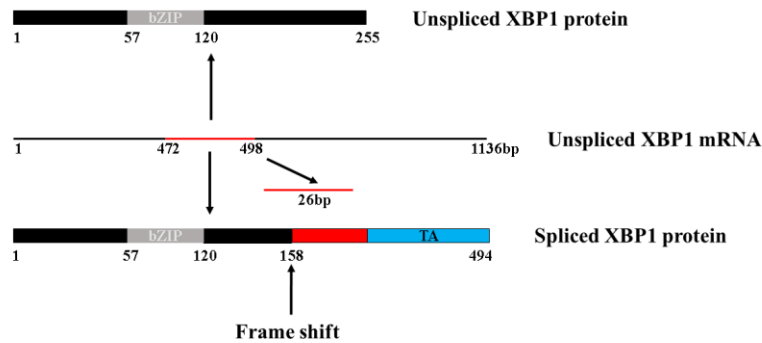


Figure 3.2: XBP1 Splicing. Unspliced chicken XBP1 mRNA has an early termination codon which upon translation produces a 255 amino acid length protein with bZIP domain but lacks transactivation domain (TA). Removal of a 26bp fragment via splicing causes a frame shift in the reading frame resulting in full length XBP1(s) protein with a transactivation domain in its C-terminus.

3.2.4 UPR and Innate Immunity

UPR pathways have been shown to induce NF- κ B activation by triggering upstream MAPKs (mitogen activated protein kinase). In macrophages, free cholesterol trafficking into the ER and induction of UPR was shown to activate MAPK (MKK3/p38, Erk1/2, and JNK1/2) signaling along with NF- κ B activation leading to TNF- α and IL-6 production (84). IRE1-TRAF2 complex has been shown to recruit I κ K complex and subsequent NF- κ B activation (157). IRE1-TRAF2 complex associates with ASK1 to promote JNK phosphorylation leading to the downstream activation of the AP1 family of transcription factors (117, 164).

In addition to NF- κ B activation, there is an association between IFN gene family activation and UPR in rheumatologic diseases including spondyloarthritis, systemic sclerosis, and specific types of myositis (43, 81, 115, 162). Cells undergoing acute UPR when treated with TLR or RLR agonists such as LPS and poly I:C, the amount of IFN β increasing tenfold due to the activation of XBP1(s) (56, 149). In addition to IFN β , UPR signaling enhances the induction of pro-inflammatory cytokines such as IL-6, TNF- α and the TH₁₇ cytokine, IL-23 (34, 102, 149).

The IRE1-dependent XBP1 transcription factor was shown to play a crucial role in the synergistic production of IFN β , ISG15, IL-6, TNF- α and IL-8 in response to combined UPR-PRR signaling (102, 104, 149, 176). ChIP studies have shown the binding of XBP1 to IL-6 and TNF- α promoters (102) and CHOP binding to IL-23p19 promoter (46). This phenomena of synergism caused by UPR-PRR stimulation was also evident upon treatment with UPR inducers such as tunicamycin or thapsigargin and PRR agonists. Synergistic cytokine production has been observed in multiple cell types including immune cells such as macrophages and dendritic cells, and was found to be cell type- and inflammatory mediator-specific (148).

3.3 Herpesviruses and UPR

It is a known fact that viruses exploit host transcriptional and translational machinery in order to produce the quantities of viral proteins necessary for viral assembly and egress. In addition, viruses utilize the host ER for folding and modifying (e.g. glycosylation) viral proteins, causing ER stress and consequently UPR activation. Viruses selectively activate UPR pathways in order to support their replication by increasing the protein-folding capacity of the ER through induced chaperone expression and metabolic regulation of cells. At the same time, deleterious effects of UPR activation on viral particle production such as translation attenuation, ERAD and apoptosis are selectively modified or repressed by viruses. Hence, selective induction, modification, or repression of UPR pathways have an important role in supporting viral replication by maintaining high-level viral protein production while maintaining, at least in the short-term, cell survival.

Expanding evidence of UPR pathways synergizing pro-inflammatory cytokine production, specifically Type I interferon production, also suggests the possibility that viruses selectively modulate UPR pathways in order to suppress anti-viral responses.

Herpes simplex virus 1 (HSV-1) selectively activates and modulates all three pathways of UPR. During HSV-1 replication, while the virion host shut-off (vhs) mechanism initially reduces the ER client load and maintains chaperone sufficiency, the sustained viral protein synthesis occurring at late stages of infection induce the UPR. High-level viral protein synthesis would lead to ER stress and subsequent UPR activation. However, the kinase domains of PERK and IRE1 remain in an inactivated state in HSV1 infected cells. This is facilitated via binding of gB onto the luminal domain of PERK, consequently inhibiting the activation of kinase domain of PERK

(110). This blocking of PERK activation by gB was also observed in the cells treated with UPR-inducer thapsigargin.

HSV1 maintains host cellular translation by selective binding and inhibition of eIF2 α kinases, PERK inactivation via early gB expression, and PKR inactivation via true late US11 (γ 2) expression. Additionally, late gene ICP34.5 (γ 1) of HSV1, via its GADD34 homology domain, mediates dephosphorylation of eIF2 α by recruiting cellular protein phosphatase PP1 α (28). Despite the lack of phosphorylated eIF2 α , HSV1-induced p-eIF2 α -ATF4 target, GADD34 expression downstream, which in turn directs PP1 α to dephosphorylate eIF2 α (28). Activation of PKR-phospho-eIF2 α signaling during infection with an HSV-1 ICP34.5 deletion mutant lead to the stimulation of autophagy. ICP34.5 also inhibits xenophagy of HSV1 virions in infected cells by binding and inhibiting Beclin-1, a regulator of autophagy (156). Recently it was shown that the US11-encoded protein also inhibits anti-viral xenophagy via PKR-binding in HSV1-infected cells during much later stages of infection, in a PKR-dependent, but Beclin-1- and mTOR-independent manner (95).

Human cytomegalovirus (HCMV) infection has been shown to induce UPR and modify the downstream consequences of all three (PERK, ATF6 and IRE1) pathways during replication (61). HCMV infection activates PERK, but limits the amount of phosphorylated eIF2 α , maintaining cellular translation. Although eIF2 α becomes phosphorylated during infection, the translation of downstream ATF4 is unaffected. This is explained by demonstrating that lower levels of phosphorylated eIF2 α is sufficient to facilitate the translation of ATF4 mRNA. In addition, HCMV early protein pUL38 was shown to induce ATF4 overexpression and inhibit JNK phosphorylation, to protect the infected cells from ER stress-induced cell death (172).

During the course of HCMV infection, ATF6 was cleaved but its activation was suppressed. However, ATF6 activation-mediated downstream target genes BiP and GRP94 were significantly induced via an ATF6-independent mechanism. Additionally, BiP cleavage and depletion by treatment of infected cells with BiP specific subtilase toxin, significantly reduced virion assembly while not significantly affecting viral protein synthesis (20). HCMV proteins US2 and US11 bind BiP to mediate degradation of MHC Class I heavy chain by direct binding and targeting it to ER associated degradation machinery in the cytoplasm (52).

Activation of the IRE1 pathway was also evident by the induction of splicing of the XBP1 mRNA. The downstream target of XBP1(s), EDEM1, however was not detected leading to a conclusion that either levels of XBP1(s) protein were low or the transcriptional activity of XBP1(s) was significantly inhibited by the virus (61).

The LMP1 (latent membrane protein 1) oncogene of Epstein Barr virus (EBV) induced all three pathways of UPR (PERK, IRE1, ATF6) in a dose dependent manner. Firstly, EBNA2 transactivates the LMP1 promoter when bound to cellular proteins RBP and PU.1. As the levels of EBNA2-induced LMP1 increase, LMP1 phosphorylates eIF2 α leading to proportional translation of ATF4. ATF4 in turn transactivates LMP1 by binding to ATF/CRE site in its promoter. This way LMP1 enhances its own induction in a positive feedback loop (80). Increasing levels of LMP1 induce more LMP1 potentiating B cell proliferation. LMP1 signals as CD40 except without a ligand. By associating with intracellular molecules, TRAF and JAK3, it activates nuclear factor- κ B (NF- κ B), AP-1, and Stat-1, promoting B cell proliferation. Although the LMP1-induced IRE1 pathway and XBP1 splicing occurs in a dose-dependent manner, EBV-infected B cells secrete immunoglobulins independent

of the levels of LMP1, suggesting that a threshold activation of XBP1 is necessary for plasma cell differentiation and Ig secretion (80).

3.4 UPR role in Tumorigenesis:

During tumorigenesis, enhanced activation of proto-oncogenes along with either loss-of-function mutations or repression of tumor suppressor genes increase protein translocation into the ER, owing to increased metabolic demand during oncogenesis. This increased protein translocation causes ER stress and subsequent UPR activation in order to enhance ER protein folding capacity.

In addition, rapidly proliferating tumor cells require UPR activation for the expansion of ER for cell division and transmission to daughter cells during proliferation. Certain types of cancers such as multiple myeloma and plasma cell malignancies express high levels of immunoglobulins and are prone to constitutive UPR activation (13, 16, 99, 136). Tumor progression also involves cancer cells co-opting immune cells such as tumor-associated macrophages (TAMs) and endothelial cells in the tumor microenvironment to facilitate tumor growth and spread. This progression also requires UPR activation to increase the folding-capacity of secretory proteins such as cytokines, growth factors, metalloproteinases, angiogenic factors, and ECM matrix components.

The tumor microenvironment is often hypoxic. Hypoxia is a direct consequence of poor vascularization of a tumorous mass outgrowing the surrounding tissue. Disulphide bond formation as part of post-translational modification or isomerization in the ER is oxygen-dependent, whereas disulphide bond formation during protein translation is oxygen-independent, which explains why hypoxic conditions induce ER stress due to mis-modified proteins (71). UPR components

ATF4 and XBP1 play an adaptive role under hypoxic conditions by enhancing HIF1 α -mediated up-regulation of its downstream target genes that promote cancer cell survival (27, 123). Anti-sense inhibition of GRP78 sensitizes the cells to hypoxia *in vitro* (85). In addition, XBP1 deficiency has been shown to reduce tumor cell survival under severe hypoxic conditions *in vitro*, and these cells were unable to grow into tumors upon transplantation due to enhanced apoptosis, thus defining the role of XBP1 as a tumor survival factor during hypoxia. Blocking integrated stress response signaling by targeting PERK significantly increases apoptosis of transformed cells under hypoxic conditions (15). Altogether UPR activation is necessary for tumor growth and progression under hypoxic conditions.

Rapid tumor development and poor vascularization of tumor mass lead to deprivation of nutrients such as glucose. Glucose deprivation leads to a loss of energy production in the form of ATP, which is the basis for sarco/endoplasmic reticulum Ca²⁺-dependent ATPase (SERCA) activity and protein biosynthesis involved in the addition of post-translational modifications, such as phosphorylation and N-linked glycosylation. Tumor cells adapt to low glucose levels by switching to increased rates of aerobic glycolysis known as the *Warburg effect* (7). This switch results in increased lactic acid production, causing a decrease in pH. The acidic tumor microenvironment facilitates tumor survival and progression via the upregulation of anti-apoptotic proteins Bcl-2 and Bcl-xL (135).

In normal cells, UPR activation in response to ER stress involves the transient attenuation of global translation, increased protein trafficking capacity associated with enhanced protein folding, and increased misfolded protein degradation through ERAD and autophagy. Under prolonged ER stress, if the adaptive mechanisms fail to restore

ER homeostasis, cells undergo apoptosis. The same principle also applies to tumor cells. UPR plays a paradoxical role in tumorigenesis by contributing to survival during acute ER stress, and apoptosis of cancer cells under prolonged ER stress. Acute UPR activation promotes adaptive mechanisms benefitting cancer cell survival, whereas during chronic ER stress, tumor cells strategically block apoptosis. However, chronic ER stress-induced cell death mechanisms are still intact in at least some tumor cells. Under persistent chronic ER stress in normal human cells, IRE1 and ATF6 pathways are attenuated, whereas PERK mediated pro-apoptotic CHOP induction is maintained (88). Some cancer cells undergoing chronic ER stress however, exhibited constitutive activation of both IRE1 α -XBP1 (19, 174) and BiP pathways, both of which are anti-apoptotic (129, 160).

3.5 Hypothesis of Research:

Given the protein encoding nature of the MDV genome and highly cell-associated nature of MDV, we hypothesized that the lytic replication of MDV is associated with induction of all three pathways of UPR, and that MDV modifies UPR signaling allowing selective activation of UPR pathways that benefit MDV replication (chaperone induction), while suppressing UPR pathways that are inhibitory to viral replication (translation attenuation, ER protein degradation components).

In a preliminary study to investigate the potential activation or selective induction of UPR during the course of MDV replication, we monitored the expression levels of downstream targets of all three UPR pathways in chicken embryo fibroblast (CEF) cultures infected with CU2, a mildly-virulent MDV1 strain at 24 hr intervals until the appearance of plaques on day 5. In follow-up to this study, we examined the induction of UPR pathways in cells infected with MDV1 strains of distinct virulence

levels. Henceforth, we examined the relative expression of UPR targets upon infection with MDV1 strains CVI988 (attenuated vaccine strain), RB-1B and Md5 (vvMDVs) and TK (a vv+MDV). We also examined these pathways in cells infected with vaccine strains (HVT and SB1) on day 5 post-infection in a separate experiment.

Given the rapid development of tumors within few weeks of infection and the T regulatory-like (T_{REG}-like) immunophenotype of lymphomas caused by MDV, we hypothesized that MDV1-mediated transformation of activated CD4⁺ T cells and lymphoma progression involves UPR activation at some level. Moreover, we also hypothesize that this UPR activation plays more of an adaptive role, rather than an apoptotic role in solid lymphomas, thereby promoting tumor cell survival, proliferation, and increased cytokine secretion, while blocking apoptosis. To investigate the role played by UPR in MDV1-induced lymphomas, we examined the relative expression of UPR targets along with the cytokine profiling in the inflammatory and proliferative solid tumor lesions isolated during a vaccine efficacy trial using commercial broiler chickens contact-exposed to vv+MDV TK strain-infected chickens, during the transformation phase at the end of the seventh week-post placement, essentially on the day of final necropsy.

3.6 Materials and Methods:

3.6.1 Cells and Viruses:

For the propagation of MDV1 serotypes and vaccine strains, secondary chicken embryo fibroblasts were prepared from 10-day-old, specific pathogen free embryos (Sunrise Farms, Inc. Catskill, NY). Secondary CEF were propagated and maintained at 37°C in 5% CO₂ in M199 medium supplemented with 3% calf serum,

L-glutamine, antibiotics (1X Penicillin/Streptomycin D/Neomycin) and antimycotics (1X amphotericin) (all reagents from Life Technologies, Carlsbad, CA).

For the preliminary time course study, cells were infected with 5000 PFU of cell-associated CU2 (a m/vMDV, obtained originally from Dr. K.A. Schat, Cornell University), in triplicate cultures for each time point, and infected CEF were harvested at 1, 2, 3, 4 and 5 days post-infection (dpi).

For experiments involving all other MDV strains (RB-1B, Md5, TK, HVT, SB1 and CVI988), CEF were infected with 5000 PFU of each strain and harvested upon the appearance of plaques on day 5. All the oncogenic viruses, CU2, RB-1B (a vvMDV, originally obtained from Dr. K.A. Schat), Md5 (originally obtained from Dr. Sanjay Reddy, Texas A & M University), and T KING (TK-2A, a vv+MDV, originally obtained from Dr. John K. Rosenberger, University of Delaware) and vaccine strains (HVT, SB-1, and CVI-988, all obtained from Merial, Inc., Gainesville, GA) described in the study were from stocks in the Parcels' laboratory.

As a positive control, SERCA inhibitor (thapsigargin) treatments were performed on CEF. Briefly, CEFs were treated in triplicates with thapsigargin (solubilized in DMSO to a final concentration of 2nM) for the indicated amount of times (1 and 3 hrs) and harvested for gene expression analysis of UPR downstream targets. As a negative control, CEF were treated with DMSO only. Expression levels from thapsigargin treated cells are based on comparison with DMSO treated cells.

3.6.2 *In vivo* Tumor Collection:

Lymphomas were isolated from commercial broiler chickens (Hubbard X Cobb) infected via contact with vv+MDV (TKING) strain of MDV-infected broilers (shedders) during a vaccine efficacy study just before necropsy (at the end of seventh

week post-placement). *In vivo* study described here employed a natural exposure model of infection known as “shedder model” that has already been described (159). Briefly, broiler chickens were inoculated intra-abdominally with 200PFU of TK on day 1 of hatch and are maintained in room equipped with wood shaving based litter, separate ventilation, feeders and waterers for 2 weeks during which they shed MDV into surroundings providing a source of highly infectious environment. At 2 weeks post placement, neck tagged unvaccinated or uninfected day old chickens were placed along with inoculated shedders. Concurrently, to serve as negative controls, uninfected or unvaccinated chickens were housed separately in a room free of infection with feed and water provided *ad libitum*.

Grossly-observable solid white spleen tumor masses (n=4) were dissected from surrounding non-tumorous spleen tissue, as described in figure 3.3 (below). In addition, as an infected control, phenotypically non-tumorous adjacent spleen sections (n=4) were collected from the corresponding tumorous spleens. To serve as negative controls, healthy normal spleens (n=4) from uninfected and unvaccinated chickens housed separately were also collected. Spleen samples were collected into RNA *later* (Ambion Inc., Austin, TX) and stored at -80°C for further RNA purification.

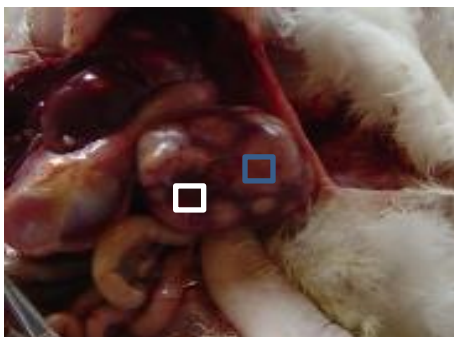


Figure 3.3: Solid white lymphoma mass (highlighted in blue square) and adjacent red non-lymphoma tissue (white square) dissected from the same spleen.

3.6.3 Quantitative RT-PCR Analysis:

Total RNA was isolated from harvested cells using the Qiagen RNA/DNA/Protein Kit, according to the manufacturer's instructions (Qiagen, USA). Total RNA quality (260/280 ratio) and quantity (at 260 nm absorbance) were measured using an Agilent Nanodrop spectrophotometer.

For cDNA synthesis, 1 µg of total RNA was reverse transcribed with random hexamers using High Capacity cDNA Reverse Transcription Kit (Applied Biosystems, USA), as recommended by the manufacturer's protocol (Step 1: 25°C for 10 min; Step 2: 37°C for 120 min; Step 3: 85°C for 5 min; Step 4: 4°C until samples are removed). Final cDNAs were diluted 10 fold and 1 µl of the diluted cDNA was used in a 20 µl reaction consisting of 10 µl iQTM SYBR[®] Green Supermix (Bio-Rad, Hercules, CA), 8.2 µl of nuclease free water and 0.4 µl (250nM) each of forward and reverse primers.

Quantitative real time PCR was performed using SYBR green chemistry as recommended by the manufacturer (Bio-rad Laboratories) on the MyiQ2 Two Color Real Time PCR Detection System (Bio-rad Laboratories, Hercules, CA). Following amplification and collection of raw fluorescence data, melt curve analysis was performed to exclude any non-specific amplification. Relative expression of target genes is based on normalization to the geometric mean of endogenous reference genes 28S ribosomal RNA and PPIB using the relative expression software tool (REST) (<http://www.REST.de.com>)

3.6.4 Primer Design:

The sequences for downstream targets of UPR signaling pathways and reference genes were obtained from ensembl (obtained from previous publications or derived from the published mRNA sequences) and primers were designed in exons

flanking introns. Primers were designed for the generation of amplicons ranging between 85-150 bp and an annealing temperature of ~58°C.

The sequence of spliced chicken XBP1 mRNA was unavailable in the databases to date. The splicing of XBP1 mRNA was evolutionarily conserved across the species from yeast to mammals with the spliced form of XBP1 having higher transcriptional activity due to the presence of a transactivation domain (175). For the prediction and quantification of spliced and unspliced XBP1, the full length chicken XBP1 mRNA sequence was aligned with that of the human, bovine, murine and xenopus ESTs using multiple sequence alignment tool CLUSTAL Omega (DNASStar). The sequence of the 26bp spliced fragment was identified in the chicken XBP1 mRNA sequence and this predicted splice site was confirmed via sanger sequencing of PCR products obtained upon treating CEFs with the SERCA inhibitor, thapsigargin.

In order to quantify the amount of unspliced and spliced XBP1, forward qPCR primers were designed in and across the splice site respectively, while a common reverse primer was designed downstream of the splice site for quantification of both spliced and unspliced XBP1. The splice sites and location of the chicken XBP1 mRNA and protein sequences are depicted in figure 2.2 (above) and Appendix A1.

3.6.5 Statistical Analysis:

Differences in gene expression levels between untreated or uninfected and thapsigargin treated or infected samples were assessed in group means for statistical significance by pair wise fixed reallocation randomization test by REST software.

3.7 Results and Discussion

3.7.1 UPR induction in MDV-infected CEFs

To determine if MDV activates PERK pathway, we determined the expression levels of ATF4 mRNA during indicated times post infection. By day 1 until day 5 post-infection, no significant changes in ATF4 expression was observed (figure 3.4). To determine whether MDV activates the ATF6 pathway, we analyzed the expression levels of activated ATF6 downstream targets, ER chaperones BiP and GRP94. No significant changes were observed among GRP78 and GRP94 expression from days 1 to 4. However, there was a significant 12-fold induction of the ER chaperone BiP on at 5 dpi (figure 3.5). Although not significant, there was a 2-fold induction of similarly-regulated target ER chaperone GRP94 (figure 3.6).

To determine if the IRE-1 pathway was activated, we quantified the amount of spliced XBP1 mRNA. No significant change in the expression levels of spliced XBP1 was observed on 1 to 4 dpi. However a significant 5-fold up-regulation of spliced XBP1 was observed on 5 dpi suggesting that MDV1 infection activated the IRE1 pathway causing splicing of XBP1 during later times of infection (figure 3.7). Once produced, the spliced XBP1 mRNA transcript is translated and localized into the nucleus where it induces the expression of chaperones (e.g. BiP, GRP94) and components of ERAD (e.g., EDEM). Since the chaperone induction is a result of activation of both ATF6 and IRE-1 pathways, we quantified the expression levels of EDEM, whose transcription is solely dependent on XBP1 (78). At 5 dpi, there was a significant induction of EDEM consistent with increased splicing of the XBP1 mRNA and confirming XBP1 mediated transcriptional activation. (figure 3.8).

One common observation upon examining the induction of UPR pathways was a lack of induction until 4 dpi and a lack of induction of ATF4 (PERK pathway) on all time points examined. MDV1-encoded or induced proteins may therefore maintain UPR signaling pathways in an inactive state during this period in order to facilitate replication and cell-to-cell spread. MDV1 is a cell-associated virus with slower *in vitro* replication kinetics. The lack of induction of ER stress/UPR signaling earlier during infection, that induces apoptosis upon prolonged activation, might be beneficial for the viral replication. On the other hand observed UPR induction on day 5 could be due to a large increase in late gene expression in a large number of cells overwhelming the normal folding capacity of ER ultimately activating UPR. Alternatively, the observed UPR induction on day 5, the day of plaque formation which is associated with cellular morphological changes (refractile rounded up or fusiform cells and actin depolymerization), could overwhelm normal folding of late structural proteins in the ER causing significant UPR activation.

Suppression of all three UPR pathways during earlier times post-infection has been demonstrated in herpes simplex virus infected cells (23). No transcriptional induction of UPR targets (ATF4, GRP78, GRP94, XBP1(s), EDEM) has been observed until 24 hr post infection in HSV1-infected cells. Earlier repression of ATF4 and XBP1(s) was suggested to facilitate replication by inhibiting phosphorylated eIF2 α -mediated global translation attenuation and ER-associated degradation, respectively, while cellular chaperone expression was thought to be sufficient to mediate proper protein-folding. Relieving this repression, and induction of CHOP or CHOP-mediated apoptosis, during the final stages of HSV1 replication facilitates

HSV1 spread by the release of enveloped virus into the surrounding medium as apoptotic bodies having multiple virus particles per vesicle.

Upon *in vitro* infection of cell associated MDV1, no significant induction of ATF4 was observed among all the time points observed, suggesting that the PERK-p-eIF2 α -ATF4 axis is maintained in an inactive state allowing viral or cellular gene translation to occur. Observed induction of BiP, GRP94, and XBP1(s) on 5 dpi likely is observed from the cells with overwhelming levels of late gene expression exceeding normal ER folding capacity, thereby activating cellular stress responses.

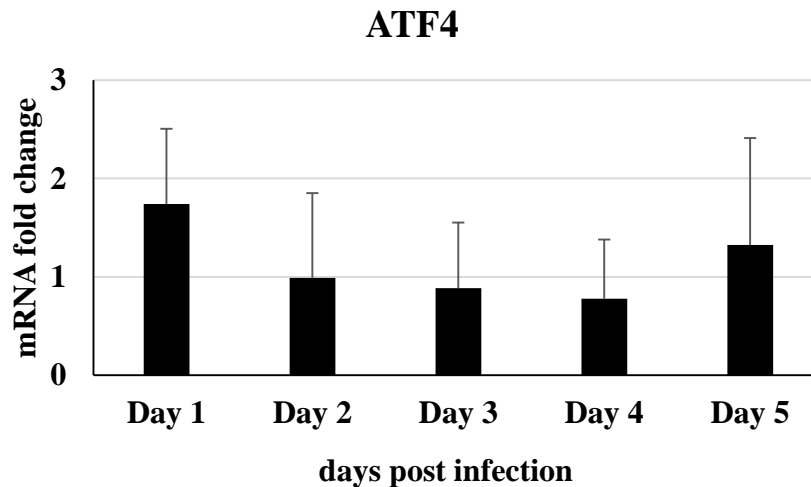


Figure 3.4: Relative expression of ATF4 in CU-2 infected CEFs. X-axis denotes fold change compared to uninfected CEFs. Y-axis denotes days post infection. Asterisk* denotes significance at $p < 0.05$ level.

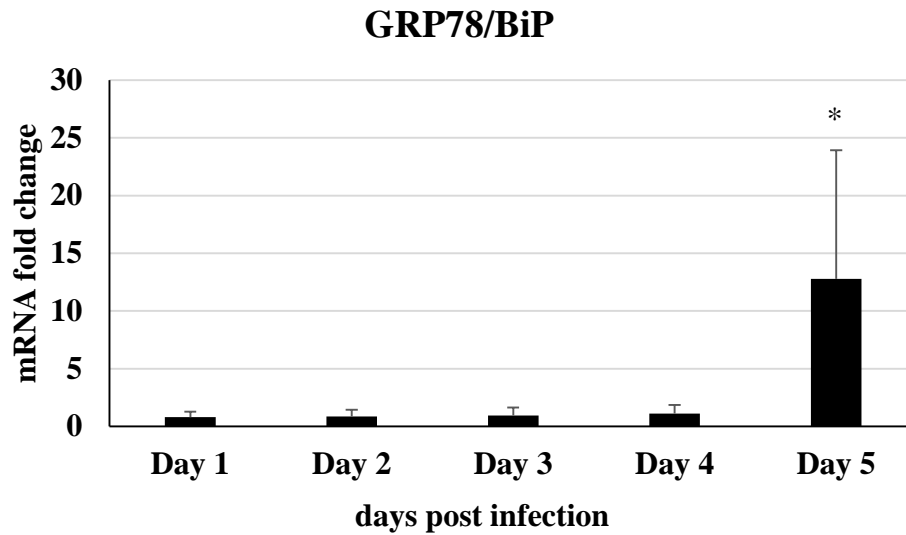


Figure 3.5: Relative expression of GRP78/BiP in CU-2 infected CEFs. X-axis denotes fold change compared to uninfected CEFs. Y-axis denotes days post infection. Asterisk* denotes significance at $p < 0.05$ level.

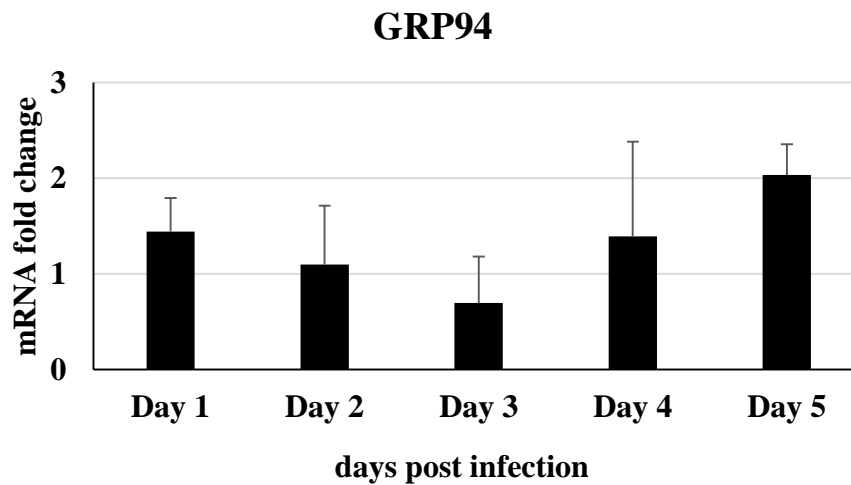


Figure 3.6: Relative expression of GRP94 in CU-2 infected CEFs. X-axis denotes fold change compared to uninfected CEFs. Y-axis denotes days post infection. Asterisk* denotes significance at $p < 0.05$ level.

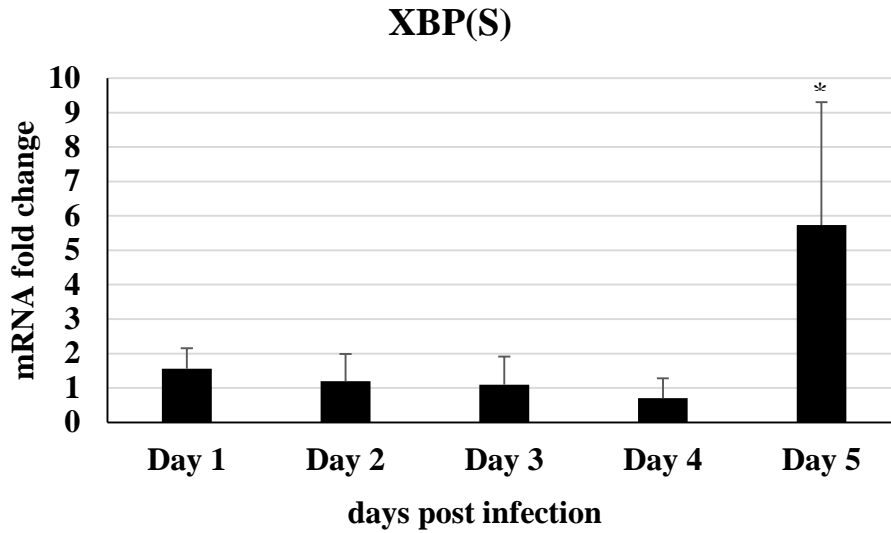


Figure 3.7: Relative expression of spliced XBP1(s) in CU-2 infected CEFs. X-axis denotes fold change compared to uninfected CEFs. Y-axis denotes days post infection. Asterisk* denotes significance at $p < 0.05$ level.

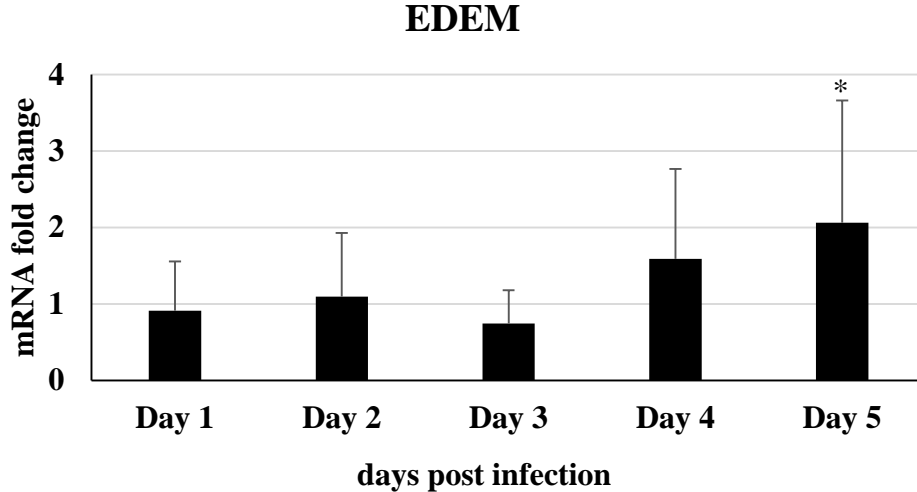


Figure 3.8: Relative expression of EDEM in CU-2 infected CEFs. X-axis denotes fold change compared to uninfected CEFs. Y-axis denotes days post infection. Asterisk* denotes significance at $p < 0.05$ level.

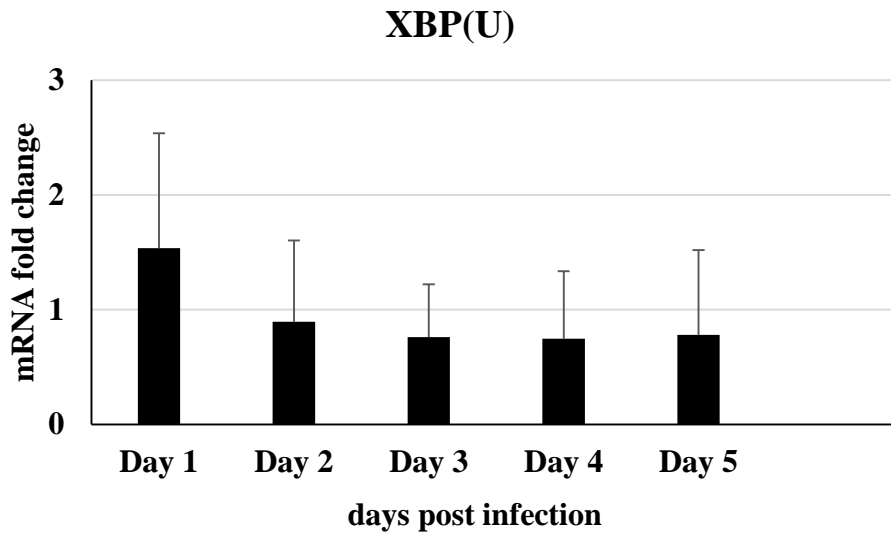


Figure 3.9: Relative expression of unspliced XBP1(u) in CU-2 infected CEFs. X-axis denotes fold change compared to uninfected CEFs. Y-axis denotes days post infection. Asterisk* denotes significance at $p < 0.05$ level.

3.7.2 Comparison of UPR induction by Vaccine and Pathogenic MDVs:

To observe any changes in the induction of UPR by different MDV strains at 5 dpi, we examined the induction of UPR by vaccine and virulence-level (pathotype) MDVs at 5 dpi. We found no significant induction of all examined UPR signaling targets by the vaccine strains at 5 dpi, an observation consistent with their high passage level and cell culture adaptation. In contrast, there was a significant induction of one or more pathways by the virulent MDV strains with profound activation of all three pathways by the vv+ MDV strain, TK. ATF4 was significantly upregulated in TK-infected cells, as well as in RB-1B- (1.76 fold) and Md5- (1.69 fold) infected cells.

Chaperone GRP78/BiP was also highly induced in TK-strain-infected cells, whereas no significant induction was observed in cells infected with very virulent

strains RB-1B and Md5. It is possible that either the levels of inherent chaperones are sufficient for the viral protein folding activity, or that the UPR sensors or their downstream effectors are more tightly regulated during infection with RB-1B and Md5 treatments.

However, another chaperone, GRP94 was significantly upregulated by very virulent strain MD5 (3.3 fold). Although not significant, there was 2.4 and 8.8 fold up-regulation of GRP94 by RB-1B and TK strains, respectively. Spliced XBP1 target gene EDEM was significantly upregulated by all strains, whereas, upstream spliced XBP1 was found significantly expressed only in TK strain-infected cells with no significant changes seen in CEF infected by RB-1B and Md5.

Finally, responses seen in TK-infected CEF were greater than in vvMDV-infected cells. The enhanced induction seen in TK strain-infected CEF, when compared to vvMDV strains might possibly be due to slow *in vitro* replicative nature of vv+MDVs, which are not adapted to CEF and tend to cause smaller plaques. In addition, the least capacity of vv+MDVs to establish productive restrictive infection in CEFs could be related to their inability to regulate early UPR sensing. Inability to regulate early UPR induction, could have a deleterious effect on viral replication posing a limit on the capacity to spread cell-to-cell and an overall decreased “burst size” (PFU per plaque) due to an inability to regulate UPR-induced apoptosis. The CU2-infected CEF expression data, however, do not support this hypothesis, at least in the case of BiP/GRP78 and XBP-1.

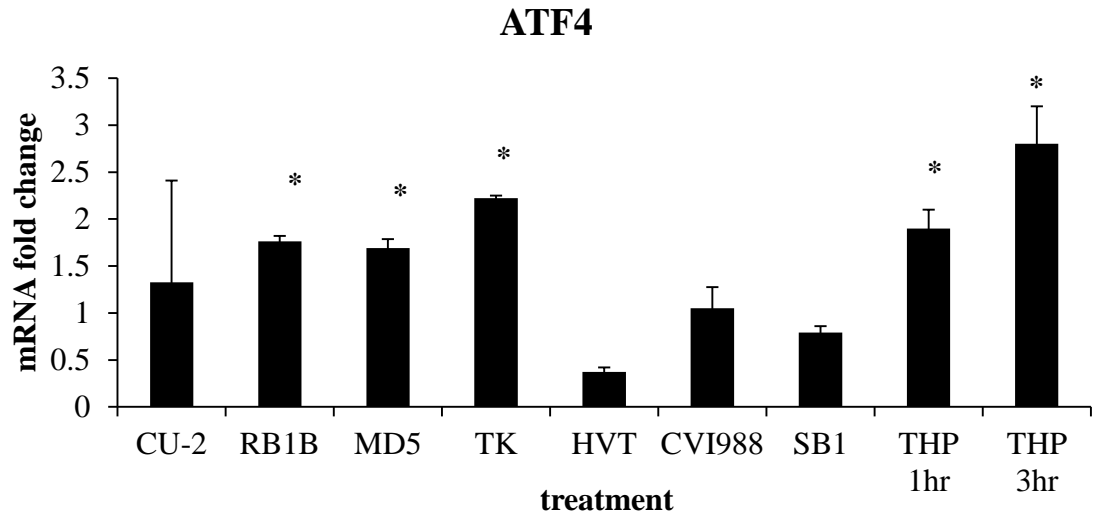


Figure 3.10: Relative expression of ATF4 among MDV1 pathotypes and vaccine strain. THP indicates thapsigargin-CEF positive treatment control. Y-axis denotes fold change compared to uninfected CEFs. X-axis denotes treatment. Asterisk* denotes significance at $p < 0.05$ level.

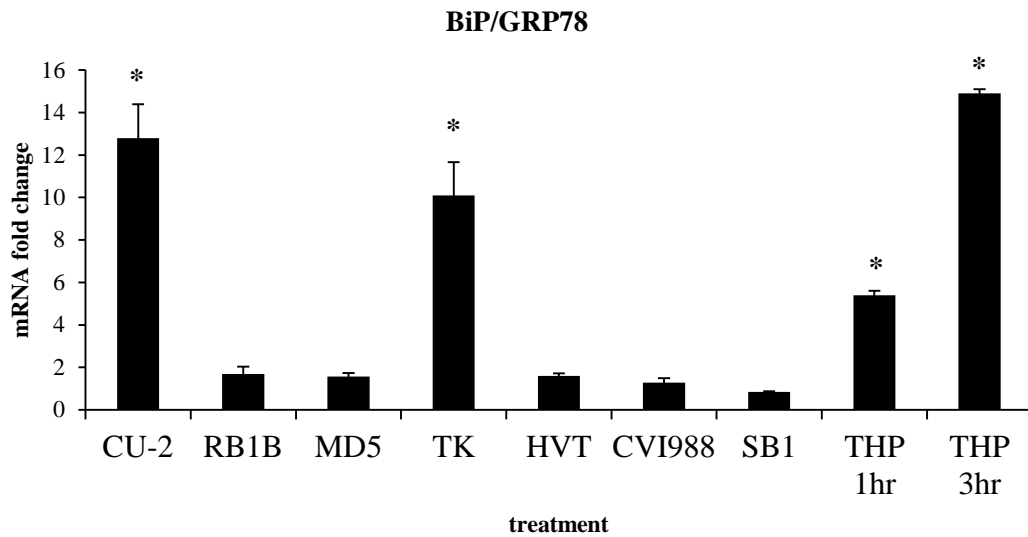


Figure 3.11: Relative expression of BiP/GRP78 among MDV1 pathotypes and vaccine strains. THP indicates thapsigargin-CEF positive treatment control. Y-axis denotes fold change. X-axis denotes treatment. Asterisk* denotes significance at $p < 0.05$ level.

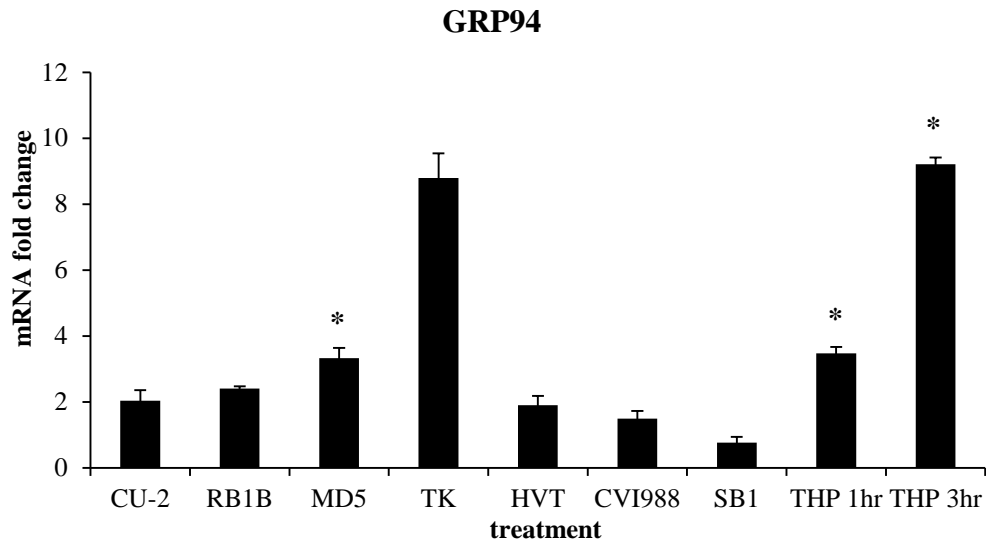


Figure 3.12: Relative expression of GRP94 among MDV1 pathotypes and vaccine strains. THP indicates thapsigargin-CEF positive treatment control. Y-axis denotes fold change compared to uninfected CEFs. X-axis denotes treatment. Asterisk* denotes significance at $p < 0.05$ level.

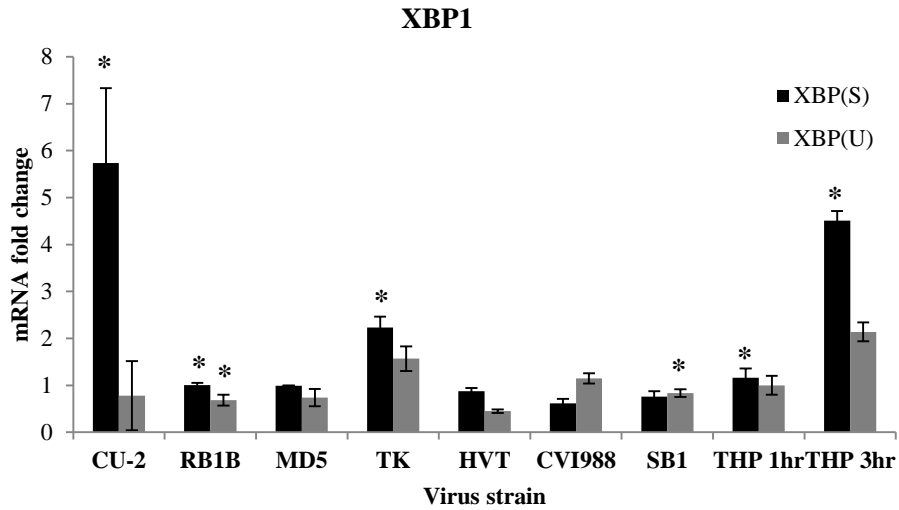


Figure 3.13: Relative expression of XBP1(s) among MDV1 pathotypes and vaccine strains. THP indicates thapsigargin-CEF positive treatment control. Y-axis denotes fold change compared to uninfected CEFs. X-axis denotes treatment. Asterisk* denotes significance at $p < 0.05$ level.

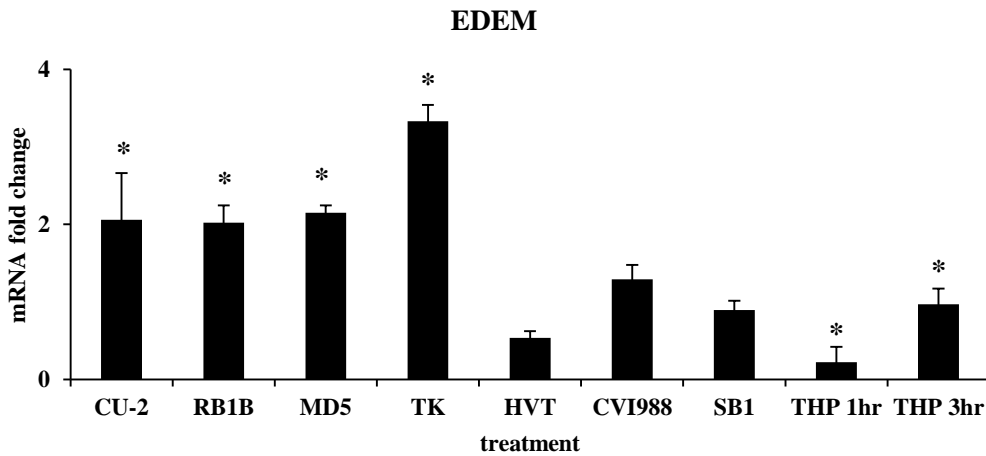


Figure 3.14: Relative expression of EDEM among MDV1 pathotypes and vaccine strains. THP indicates thapsigargin-CEF positive treatment control. Y-axis denotes fold change compared to uninfected CEFs. X-axis denotes treatment. Asterisk* denotes significance at $p < 0.05$ level.

3.7.2 UPR Induction *in vivo* in TK-Induced Lymphomas

Solid lymphomas are heterogenous mixtures composed of minor MD transformed CD3⁺, CD4⁺, MHC-I^{hi}, MHC-II^{hi}, CD25^{lo} and CD28^{hi/-} T_{reg}-like component surrounded by a major non-transformed component constituting highly inflammatory tissue (21, 75). The non-transformed tissue component is mainly composed of immune (pro- or anti-inflammatory) cells such as T helper cells (T_{H1}, T_{H2}, T_{H17}), B cells, tumor-associated macrophages and non-immune tissue specific cells or stromal endothelial cells (75). The transformed component depends upon the local lymphoma microenvironment for their survival, proliferation, and growth (75). On the other hand cell lines established from MD lymphomas represent transformed component and are tumorigenic when re-injected *in vivo*. To confirm the integrity of lymphoma tissue to corresponding adjacent, visibly normal, tissue dissected from the same spleen, we analyzed the expression level of the oncogene *meq* which is directly associated with MDV-transformation of activated CD4⁺ T cell and is highly expressed in CD30^{hi} cells. The Meq expression level was 34 fold higher in the dissected lymphoma tissues compared to adjacent, phenotypically-normal tissue from the same spleen (Fig 4.1).

Additionally, we compared the target gene expression levels in solid tumor tissues to healthy spleen tissue isolated from unvaccinated and uninfected chickens housed separately. The expression trends of target genes were no different in either case except for *XBPI(s)* and *(u)*, although this was not significant (Fig 3.16). To confirm the integrity of adjacent non-tumorous tissue dissected from tumor spleens, we compared the target gene expression levels in non-tumorous tissue to healthy spleen tissues and found no significant differences.

Among the UPR targets analyzed in TK-induced lymphomas, there was a significant upregulation of ER chaperone GRP94 when compared to adjacent tissue (Figure 3.16). Although not significant, there was a transcriptional induction of ER chaperone GRP78/BiP and XBP1(s). Both GRP94 and BiP are transcriptionally regulated mainly by ATF6 and XBP1(s) (78). Based on the transcriptional induction of these targets, ATF6 and IRE1 pathways might play an active role in the UPR induction and maintenance during lymphoma progression.

ATF6-GRP94, GRP78/BiP, and IRE1-XBP1 pathways generally play a cytoprotective role in the transformed and surrounding inflammatory cells given the adaptive and anti-apoptotic roles played by ATF6 and IRE1-XBP1(s) axes, respectively. No significant induction of ATF4 was observed in our study, indicating that the PERK pathway is not induced in this context or may be actively repressed. PERK repression could possibly maintain active translation in lymphoma masses necessary for the proliferation and maintenance of tumor cells and the surrounding inflammatory environment. Moreover, a lack of PERK-ATF4 induction would prevent ATF4 downstream CHOP/GADD153/DDIT3-mediated apoptosis in the tumor cells, possibly contributing to cell survival and lymphoma progression.

ATF4/CHOP heterodimers mediate transcriptional induction of genes involved in the UPR, autophagy, and mRNA translation leading to increased protein synthesis (49). Consequently, CHOP-mediated increased protein synthesis causes ATP depletion, protein misfolding, and oxidative stress-induced cell death. More importantly, the bZIP domain of human DDIT3, a bZIP transcription factor belonging to C/EBP family, known to cause G1 cell cycle arrest or inhibit cellular proliferation, migration (63) and promote ER stress or hypoxia induced apoptosis (14, 96, 103) was

shown to interact with the *meq* bZIP domain in solution (130). However, DDIT3 does not form heterodimers with AP-1 family, while it does enhance AP-1 transcription via interaction with AP-1 complexes without binding to DNA itself (163).

Chaperones GRP78 and GRP94 are mainly localized in the ER based on their ER retention sequences (KDEL) at their C termini. In the ER, they mainly function to promote protein folding, secretion, degradation in addition to maintenance of Ca²⁺ homeostasis. Overexpression of GRP78 and GRP94 proteins has been observed in numerous cancers such as breast, colorectal, esophageal, gastric, head, neck, liver, lung and multiple myeloma (79). Increased GRP78 and GRP94 were observed with RSV-mediated cellular transformation of CEFs and rat kidney cells (151).

In cancer, overexpressed GRPs translocate to various other cellular compartments due to saturation of KDEL receptors in the ER and mediate a diverse range of functions (116). Overexpressed GRPs, upon translocation to other cellular compartments, assume novel functions that control signaling, proliferation, apoptosis, invasion, inflammation, and immunity (79). In addition, GRPs are also secreted from cells and were identified in the plasma of cancer patients.

As ER chaperones, GRP78 and GRP94 promote processing and maturation of numerous cell surface receptors and secretory proteins that are crucial for cancer cells to mediate extrinsic proliferative signals. On the cell surface, GRP78 and GRP94 mainly exist as peripheral proteins via interaction with other cell surface proteins. Cell surface expressed GRP78 was found to colocalize with PI3K which mediates PIP2 conversion to PIP3 to promote AKT activation, sustained proliferation, survival signaling, and migration (47, 89, 92, 125, 178, 179). Additionally, GRP78 was also a downstream target of insulin growth factor-PI3K signaling in cancer cell lines,

contributing to a positive feedback loop for GRP78 expression and cell proliferation. Cell surface GRP78 functions as co-receptor for kinases such as AKT, FAK, PAK2 mediating tumor cell motility. GRP94 controls the maturation and production of insulin-like growth factors (IGFs) that bind to IGFR1 and activate PI3K-AKT axis, inducing mitogenic proliferation (167). Similarly, overexpressed GRP94 also influences cell migration indirectly via its interaction with ECM and cellular interaction components, such as integrins, in the ER in order to mediate proper folding. Upon knockdown of GRP94, the Wnt-LRP-survivin pathway was inhibited in human multiple myeloma, resulting in apoptosis of cancer cells defining the pro-survival or pro-proliferative actions of GRP94 in human multiple myeloma (57).

Along with their proliferative functions, GRP78 and GRP94 are in general anti-apoptotic (93). GRP78 complexes with caspase 7, an ER-localized executioner caspase, protecting cells from apoptosis. GRP78 and BCL2 form distinct complexes with the pro-apoptotic mitochondrial channel protein BIK. BCL2-BIK complex sequestration reduces BCL2 interaction with ER causing ER Ca^{2+} release. Ca^{2+} released from ER and up taken by ER associated mitochondrial membranes can cause a collapse in inner mitochondrial membrane potential causing an activation of intrinsic pathway of apoptosis (39, 181). In cancer cells, over expressed GRP78 sequesters BIK removing the inhibition on anti-apoptotic BCL2, contributing to cell survival. Nuclear localization and DNA cross-linking of GRP78 has been reported to suppress DNA damage-induced apoptosis through a less understood mechanism (177). ER stress causes mitochondrial localization of GRP78, which upon interaction with Raf1, inhibits ER-stress induced apoptosis by maintaining mitochondrial homeostasis (147).

GRP94 protects cancer cells from apoptosis by maintaining ER Ca^{2+} homeostasis (128). GRP94 promotes production of anti-oxidants to neutralize ROS produced under hypoxia or oxidative stress in cancer cells and also facilitates disulfide bond formation in proteins.

Overexpressed GRPs were also observed as being expressed in endothelial cells in the tumor microenvironment, contributing to pro-angiogenic functions necessary for tumor cell survival. In the context of MDV-induced lymphomas, an increased level of GRP78 and GRP94 might possibly play a similar functional role as in other cancers. GRP78 shares 65% homology with its cytoplasmic analogue, Hsp70, which has been shown to interact with the Meq oncoprotein and localize to the nucleus (180). Cell surface expression of GRP78 on T cells complexes with $\text{TGF}\beta$, conferring stabilization and induction of the T regulatory immunophenotype, suppressing the $\text{T}_{\text{H}1}$ response against tumor cells (118).

Finally, although not statistically-significant, there was a trend towards increased expression of spliced XBP1. Enhanced XBP1 splicing has been demonstrated in numerous hematological malignancies and solid tumors, such as B cell lymphomas, adenomas, and adenocarcinomas, respectively (31, 40, 99). Overexpression of XBP1(s) is observed in malignant phenotypes with poor survival rates. Loss of XBP1 has been shown to inhibit tumor growth and blood vessel formation.

In general, the IRE1-XBP1(s) axis has an overall anti-apoptotic effect on BCL2 family members, facilitating cancer cell survival, while the IRE1-JNK axis has a pro-apoptotic effect. We observed no significant increase in the XBP1(s) downstream target gene, EDEM, however, in TK induced lymphomas. This protein is

associated with protein degradation and may be expected to be upregulated during vv+MDV infection. In the lymphomas, however, in which the MDV genome is maintained in a latent state and is largely repressed, a lack of EDEM induction is not particularly surprising. Moreover, TK-induced lymphomas have been described previously as being highly proliferative, overgrowing their blood supply, inducing necrotic centers within lymphomas and causing “donut-shaped” lymphomas in visceral organs (E. Montiel, MS Thesis, UD).

It should be noted, however, that the TK strain used in this study corresponds to the TK-2A variant, which does not possess a mutation (a 12nt deletion) in the coding sequence of gL, but does have two additional Meq mutations corresponding to somewhat higher virulence MDVs (648A, 660, 686, U, N strain) (158). TK-2A has a proline at position 277 as opposed to lysine in TK-1A. Consequently, there may be a different tumor phenotype, in terms of UPR gene expression, between the TK used in this study (TK-2A), and the original TK strain described in the early 1990s (TK-1A).

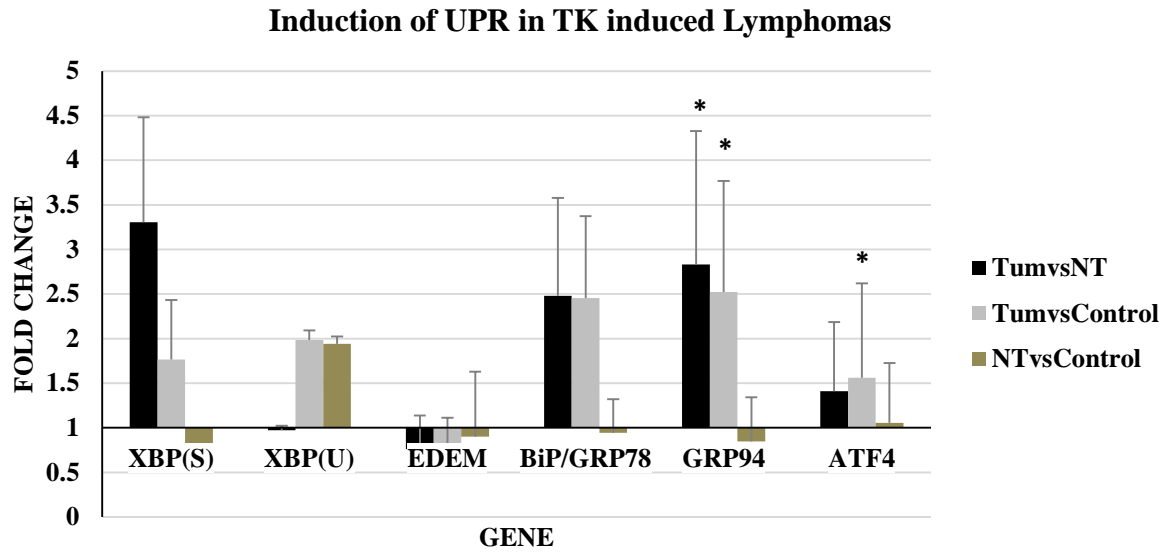


Figure 3.15: Relative expression of UPR target genes in TK induced lymphoma. X-axis denotes respective gene targets. Y-axis denotes relative expression levels or fold changes. Asterisk* denotes significance at $p < 0.05$ level. TumvsNT denotes expression levels in lymphomas compared to non-tumorous part of same spleen. TumvsControl denotes expression levels in lymphomas compared to healthy control spleens (uninfected or unvaccinated). NTvsControl denotes expression levels in non-tumorous spleens compared to healthy control spleens (uninfected or unvaccinated).

CYTOKINE COMPOSITION OF TK INDUCED SOLID LYMPHOMAS

4.1 Introduction:

MDV1 induced lymphomas serve as an excellent animal model to study fundamental mechanisms of herpesvirus oncology and complex dynamics of host-tumor interactions. Since the identification and isolation of neoplastically transformed cells in MDV1 induced lymphomas, many studies have focused on factoring key steps involved in tumor initiation and progression by utilizing various approaches. With the increase in the availability of chicken lymphocyte antigen specific monoclonal antibodies, studies in our lab and by others examined the surface antigen expression and activation status of either MD derived lymphoblastoid cell lines or lymphoma cells *ex vivo*. Based on those studies, cell lines established from highly virulent strains tend to have atypical phenotype. As an example, MDCC-UD33 and MDCC-UA51, both established from TK spleen lymphoma have the following phenotypes respectively, CD3⁻, CD4⁻, CD8⁻, CD8β⁻, (TCR1, 2, 3)⁻, CD28⁻, K55⁻, MHCII⁺, CD45⁻, IgM⁻, Bu⁻ and CD3⁻, CD4⁻, CD8⁻, CD8β⁻, TCR1⁻, TCR2⁺, TCR3⁻, CD28⁺, K55⁻, MHC-II⁺, CD45⁻, IgM⁻, Bu⁻. The only indicative immune phenotype that specifies these cells being T cells is the surface expression of CD28 activation antigen. On the other hand, Shack *et al.*, 2008 have profiled cytokines specific to various T helper cell subsets (T_{H1}, T_{H2}, T_{REG}) at transcript and protein levels in CD30^{hi/lo} cells derived from GA/22 induced lymphomas in various organs and sorted *ex vivo*. Another study from the same group profiled cytokines specific to various T helper cell subsets (T_{H1}, T_{H2}, T_{REG}) in whole tissue and tumor microenvironment of GA/22

induced kidney lymphomas in line 6₁ (resistant) and 7₂ (susceptible) chickens and reported that fundamental differences exist at the level of tissue immune response but not at the level of transformed cells. A pro-CTL response was found to exist in the tissue environment of resistant chickens. Both the studies were performed in SPF chickens infected with virulent strain at day 14 post hatch. To date, no study has investigated cytokine de-regulation by vv+ MDV1 strains that contributes to tumor initiation and progression. Very virulent plus strains show increased *in vivo* replication rates and induce sustained levels of immune suppression early in infection, profound stunting and distinctive neurological lesions. In addition, they cause higher incidence of lymphomas in adult chickens. In the current study, we profiled cytokines at the transcript levels using qRT-PCR in the spleen lymphomas isolated from commercial broiler chickens that are naturally exposed via contact on day 1 post hatch with vv+ TK2a variant.

4.2 Hypothesis of Research:

Since the cell lines established from vv+MDV1 tend to have an aberrant surface immune phenotype, and tissue specific changes associated with very virulent plus MDV1 induced lymphomas have never been investigated, we were determined to examine gene expression changes associated with vv+ MDV1 induced lymphomas. Investigating the inherent cytokine networks would establish a more plausible rationale on factors contributing to lymphoma progression by highly virulent MDV1 strains. Since our study is based on examining gene expression changes in solid lymphoma tissues that comprise heterogeneous mixtures of transformed and inflammatory (pro- or anti-) we hypothesized that responses might involve more than mere T_{H2} or transformed T_{REG} responses described in other studies.

4.3 Materials and Methods:

Much of the experimental materials and methods employed for the current study are described in Chapter 3, section 3.6.2 under *in vivo* tumor tissue collection and section 3.6.3 of this thesis. Briefly, frank lymphoma masses were dissected from the spleens of commercial broiler chickens at the end of seventh week post hatch. Concurrently, visibly normal tissue from the same spleen was also dissected into RNA *later* (Ambion Inc.,) for RNA isolation and qRT-PCR analysis. Relative expression of target genes signifying various T helper cell subsets is based on comparing transcript levels from lymphoma masses to visibly normal tissue from the same spleen. Target genes are normalized to geometric mean of reference genes 28S RNA and PPIB. Primer sequences for the target genes included in the study are mentioned under Appendix A.

4.4 Cytokine Profiling of TK Induced Lymphomas

In regards to the transcription profiling of cytokines in vv+ lymphomas, there was a significant up-regulation of IFN- γ (29.9 fold), IL-2 (21.7 fold), IL-4 (23.75 fold), IL-10 (48.58 fold), IL-17 (21.89 fold), IL-21 (20.64 fold), TGF β 2 (14.95) and IL-6 (15.37 fold) (Figure: 4.1). Further, there was a significant up-regulation of T_{H1} signature transcription factor T-bet (3.7 fold), with no significant change in the T_{H2} – associated transcription factor, GATA3 (0.86 fold).

NK cells and CTLs are implicated in anti-tumor immunity against MD. To monitor the infiltration of anti-tumor CD8+ cytotoxic T cells and NK cells in the lymphoma tissue environment, we examined the expression levels of FasL which was found to be significantly up-regulated (19.46 fold). IL-2 and IFN- γ are ostensibly expressed by infiltrated CD4+ T_{H1}-polarized cells in the solid tumors. IFN- γ functions

through activation of STAT1 resulting in the transcriptional induction of Tbx21 gene and T-bet. T-bet in turn upregulates IFN- γ in a positive feedback loop resulting in T_{H1} differentiation.

IL-2, a T cell growth factor essential for proliferation and activation, also upregulates T-bet resulting in efficient stabilization and maintenance of T_{H1} lineage (87). Consistent with this, we found an up-regulation of T-bet (3.7 fold). IFN- γ secreted by T_{H1} cells enhances cytotoxic properties of CD8⁺ CTLs, as demonstrated by the upregulation of FasL, although transformed cells are typically resistant to cytotoxic effects via down-regulation of Fas by Meq (82).

One study based on microarray analysis of spleen tumors isolated from vMDV (GA strain)-infected birds during the late transformation phase (31-56 dpi) showed no differential expression of IFN- γ and IL-6 when compared to control spleens (86). Another study, based on comparing cytokine profiles in CD30^{hi} to CD30^{lo} cell populations from GA/22 induced MD lymphomas reported an increase in IFN- γ mRNA and protein levels in CD30^{hi} compared to CD30^{lo} populations (145). More recently, *in vivo* down regulation of IFN- γ via rAAAV expressing shRNA, did not affect MD vaccine efficacy, suggesting that IFN- γ is not in and of itself associated with resistance or anti-tumor responses(50). Our observed association between IFN- γ expression and T cell transformation may be due to the pathotype virus used for infection and also stage of transformation at which the tissues are collected.

Alternatively, the expression of IFN- γ may be associated with the chicken T cell transformation process, itself. Chicken T cells transformed by reticuloendotheliosis virus, type T (REV-T), for instance, were used for the cloning of the chicken IFN- γ gene (36). In the case of MDV, transformed T cells may express

IFN- γ as a mechanism for the maintenance of latency, as this cytokine was shown previously to inhibit MDV lytic infection (171).

In our study, we found a significant induction of T_{H2} cytokine, IL-4, with no induction of GATA3, suggesting a GATA3-independent IL-4 induction mechanism. The IL-4-activated, STAT6 pathway drives T_{H2} differentiation by upregulating GATA3. However IL-2 has also been reported to constitutively activate STAT5 and promote its binding to the IL-4 promoter without upregulating GATA3, which might be a possible mechanism of action (30). In addition, the transformed component of MDV-induced lymphomas are CD30^{hi} and CD28^{lo} with a skewing towards a T_{reg}-like immunophenotype (145), and IL-4 induces CD30 expression on the surface of activated T cells, even in the absence of CD28 co-stimulation (44). The presence of IL-4 produced either by macrophages (M2) or T_{H2} cells during the earlier, cytolytic phase could possibly act on the activated CD4⁺ cells to induce higher levels of CD30 in addition to *meq*-induced CD30 contributing to tumor initiation and lymphoma progression.

One novel observation in our study was a significant induction of T_{H17}-associated cytokines IL-17 and IL-21, along with IL-6 and TGF β in the lymphoma milieu. High frequency infiltration of T_{H17} cells in the tumor microenvironment has been observed in human prostate, breast, ovarian and gastric tumors (73, 105, 144, 182). Mammalian T_{H17} differentiation is driven upon TCR stimulation of naïve CD4⁺ T cells that are also co-stimulated with IL-6, IL-1 β and TGF β , while IL-21/23 maintains their long term persistence (72, 152). TGF- β induces IL-6R α and aids in maintaining responsiveness of T cells to IL-6. In mammals, IL-6 functions by STAT3 activation and subsequent ROR γ t induction, promoting T_{H17} differentiation. In

addition, IL-6 is also a strong inducer of IL-21 via STAT3 directly, without induced ROR γ expression (154). However the functionality of ROR γ orthologs has yet to be identified in chickens. Apart from ROR γ t, CHIP-seq studies in mice have identified a range of transcription factors bound either co-operatively or competitively at IL-17 and IL-21 promoters in T_{H17} cells, such as STAT3, BATF, IRF4, c-MAF, c-JUN/JUN-B/JUN-D and Fra-2 (29). Since we have not investigated the presence of these cytokines at the protein level, and the cell type secreting these cytokines, it's a difficult task to interpret the role played by these cytokines.

T_{H17} cells are mainly implicated in autoimmune disorders and immune responses to extracellular bacteria or fungi. T_{H17} cells have been shown to play a dual role in the tumor microenvironment promoting inflammation, VEGF-induced angiogenesis, tumor growth and metastasis in some cases, while suppressing tumors by potentiating effector functions of anti-tumor CTLs and innate effectors such as NK cells, macrophages and neutrophils in others (12, 113).

In mammals, TGF- β is a common player in inducing pro-inflammatory T_{H17} cells and anti-inflammatory iTregs. The balance between T_{H17} and iTreg cells is dependent upon the induced expression of ROR γ t and Foxp3 and their association with each other, whose functional presence has not been established in the chicken.

Given the highly immunosuppressive T reg-like phenotype of MD lymphomas with an enhanced expression of deregulated self-antigens on their surface, a distinct subset of IL-17 secreting T_{H17} or CD8⁺ T cells (Tc17) might be a possibility, due to the presence of IL-6 and TGF- β in lymphoma environment. Activated T cells or monocytes express CD30L (CD153), but neither B cells nor CD30^{hi} cells express this ligand, or at least this has not been demonstrated. CD30:CD30L signaling executed

via activated T- naïve T cell interaction was demonstrated to promote Th17 differentiation by reverse signaling via CD30L downregulating IL-2, suggesting the possibility of distinct T_{H17} subsets induced by CD30^{hi} transformed Tregs at much later stages of infection (153). Another possibility might be, given the plasticity of T cells in malignant lymphomas, and recent evidence of T_{H1}/ T_{H17} and intermediary T_{H17}/Treg phenotypes, it is possible that these cytokines are induced by either by transformed Tregs or anti-tumor CD4⁺ T_{H1} cells responding to cytokines in the lymphoma environment.

Finally, there was a significant up-regulation of IL-10 and TGF- β , indicators of the T regulatory immunophenotype seen in MD lymphomas. Apart from IL-10 and TGF- β , IL-2 plays an important role in the maintenance of T regulatory cells at the same time inhibiting the percentage of T_{H17} cells (74). IL-2 acts via the high affinity IL-2R complex (CD25) containing α , β and γ chains, resulting in activation of STAT5 and subsequent induction of IL-10. In fact, avian CD4⁺CD25⁺ T_{regs} sequester IL-2 secreted by other cells in order to mediate their suppressive action and avian CD4⁺CD25⁺ T regs have no detectable IL-2 mRNA. Based on vIL-8 mediated recruitment of CD4⁺25⁺ T cells, these cells might be actual target cells for infection and transformation. Alternatively, they might be recruited to mediate suppressive responses against anti-tumor immunity during initial phases of transformation. In either case, transformed MD cell lines display low level surface expression of CD25 α (IL-2R α) (121, 124), and MDV is thought to subvert IL-2R signaling, resulting in immortalization and transformation indicating an IL-2-independent transformed T_{reg} phenotype. The role played by IL-2 in MDV transformation is unknown, although its intracellular expression was found in the MSB1 cell line, the CD30^{hi} transformed

component of RB-1B-induced primary lymphomas, and the IL-2 promoter was found to bind Meq/c-Jun heterodimers, *in vitro* and *in vivo* (83).

Alternatively, since MDV-induced lymphomas are complex mixtures of apparently pro-inflammatory and anti-inflammatory components, it is plausible that the recruitment of M1-polarized macrophages to latently-infected and immortalized T cells may open genetic loci in these T cells through inflammatory cytokine signaling. For instance, the CD30 locus is tightly regulated in T cells and requires epigenetic changes for it to become accessible to transcription factors (e.g., SAT1B). Therefore, lymphoma formation may be a sequential process, involving establishment of latency, recruitment of inflammatory components and subversion of this inflammation to proliferation and cellular survival, with recruited inflammatory cells providing essential loci-altering signals in latently-infected T-cells leading to full oncogenic transformation.

Based on the transcriptional induction of the cytokines in the lymphoma milieu, it appears that the following cell populations are present in the tumor environment: T_{H1} (IFN- γ , T-bet) T_{H2} (IL-4), T_{H17} (IL-17, IL-21, TGF- β) and transformed Treg (IL-4, TGF- β , IL-10). STATs and various other cytokine inducing transcription factors belonging to NF- κ B/AP-1 family are implicated in inducing these cytokines. However, the anti-tumor immune regulated or transformed deregulated role played by these STATs or AP-1 family transcription factors is unknown and can be more fully understood by deciphering their activation status as *ex vivo*-sorted tumor cells, or as MD lymphoblastoid cell lines.

Investigation of cytokine networks provides a definitive basis in factoring key steps involved in shaping the tumor-initiating environment and subsequent lymphoma

progression. In addition, the rapid formation of T cell lymphomas by MDV serves as an excellent model for designing and testing targeted therapeutics such as recombinant cytokines or small molecule inhibitors that are able to alter the cytokine milieu, causing a shift in the initial tumor promoting events or targeted elimination of transformed T cells.

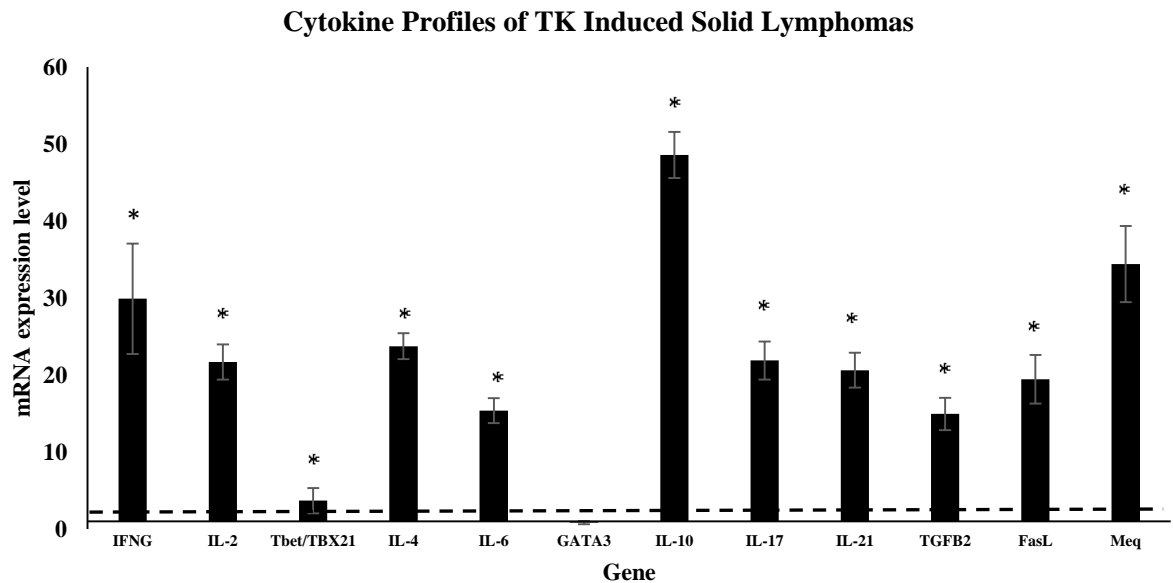


Figure 4.1: Relative expression of T-helper cell signature cytokines and transcription factors in TK lymphomas. Y-axis denotes fold change in tumorous tissue compared to adjacent non-tumorous tissue. X-axis denotes treatment. Dotted line represents 2 fold change in relative mRNA expression level. Asterisk* denotes significance at $p < 0.05$ level.

REFERENCES

1. **Abdul-Careem MF, Hunter BD, Lee LF, Fairbrother JH, Haghighi HR, Read L, Parvizi P, Heidari M, Sharif S.** 2008. Host responses in the bursa of Fabricius of chickens infected with virulent Marek's disease virus. *Virology* **379**:256-265.
2. **Abdul-Careem MF, Hunter BD, Nagy É, Read LR, Sanei B, Spencer JL, Sharif S.** 2006. Development of a real-time PCR assay using SYBR Green chemistry for monitoring Marek's disease virus genome load in feather tips. *Journal of virological methods* **133**:34-40.
3. **Abdul-Careem MF, Hunter BD, Parvizi P, Haghighi HR, Thanthrige-Don N, Sharif S.** 2007. Cytokine gene expression patterns associated with immunization against Marek's disease in chickens. *Vaccine* **25**:424-432.
4. **Abdul-Careem MF, Hunter BD, Sarson AJ, Parvizi P, Haghighi HR, Read L, Heidari M, Sharif S.** 2008. Host responses are induced in feathers of chickens infected with Marek's disease virus. *Virology* **370**:323-332.
5. **Abdul-Careem MF, Hunter DB, Lambourne MD, Read LR, Parvizi P, Sharif S.** 2008. Expression of cytokine genes following pre- and post-hatch immunization of chickens with herpesvirus of turkeys. *Vaccine* **26**:2369-2377.
6. **Abdul-Careem MF, Read LR, Parvizi P, Thanthrige-Don N, Sharif S.** 2009. Marek's disease virus-induced expression of cytokine genes in feathers of genetically defined chickens. *Developmental and comparative immunology* **33**:618-623.
7. **Amann T, Hellerbrand C.** 2009. GLUT1 as a therapeutic target in hepatocellular carcinoma. *Expert opinion on therapeutic targets* **13**:1411-1427.
8. **Andersen CL, Jensen JL, Orntoft TF.** 2004. Normalization of real-time quantitative reverse transcription-PCR data: a model-based variance estimation approach to identify genes suited for normalization, applied to bladder and colon cancer data sets. *Cancer research* **64**:5245-5250.
9. **Anobile JM, Arumugaswami V, Downs D, Czymmek K, Parcels M, Schmidt CJ.** 2006. Nuclear localization and dynamic properties of the Marek's disease virus oncogene products Meq and Meq/vIL8. *Journal of virology* **80**:1160-1166.
10. **Baaten BJ, Staines KA, Smith LP, Skinner H, Davison TF, Butter C.** 2009. Early replication in pulmonary B cells after infection with Marek's disease herpesvirus by the respiratory route. *Viral immunology* **22**:431-444.
11. **Baigent SJ, Petherbridge LJ, Howes K, Smith LP, Currie RJW, Nair VK.** 2005. Absolute quantitation of Marek's disease virus genome copy number in

- chicken feather and lymphocyte samples using real-time PCR. *Journal of virological methods* **123**:53-64.
12. **Bailey SR, Nelson MH, Himes RA, Li Z, Mehrotra S, Paulos CM.** 2014. Th17 cells in cancer: the ultimate identity crisis. *Frontiers in immunology* **5**:276.
 13. **Balague O, Mozos A, Martinez D, Hernandez L, Colomo L, Mate JL, Teruya-Feldstein J, Lin O, Campo E, Lopez-Guillermo A, Martinez A.** 2009. Activation of the endoplasmic reticulum stress-associated transcription factor x box-binding protein-1 occurs in a subset of normal germinal-center B cells and in aggressive B-cell lymphomas with prognostic implications. *The American journal of pathology* **174**:2337-2346.
 14. **Barone MV, Crozat A, Tabaee A, Philipson L, Ron D.** 1994. CHOP (GADD153) and its oncogenic variant, TLS-CHOP, have opposing effects on the induction of G1/S arrest. *Genes & development* **8**:453-464.
 15. **Bi M, Naczki C, Koritzinsky M, Fels D, Blais J, Hu N, Harding H, Novoa I, Varia M, Raleigh J, Scheuner D, Kaufman RJ, Bell J, Ron D, Wouters BG, Koumenis C.** 2005. ER stress-regulated translation increases tolerance to extreme hypoxia and promotes tumor growth. *The EMBO journal* **24**:3470-3481.
 16. **Boelens J, Jais JP, Vanhoecke B, Beck I, Van Melckebeke H, Philippe J, Bracke M, Jardin F, Briere J, Leroy K, Offner F, Lust S.** 2013. ER stress in diffuse large B cell lymphoma: GRP94 is a possible biomarker in germinal center versus activated B-cell type. *Leukemia research* **37**:3-8.
 17. **Brown AC, Baigent SJ, Smith LP, Chattoo JP, Petherbridge LJ, Hawes P, Allday MJ, Nair V.** 2006. Interaction of MEQ protein and C-terminal-binding protein is critical for induction of lymphomas by Marek's disease virus. *Proceedings of the National Academy of Sciences of the United States of America* **103**:1687-1692.
 18. **Brown MS, Ye J, Rawson RB, Goldstein JL.** 2000. Regulated intramembrane proteolysis: a control mechanism conserved from bacteria to humans. *Cell* **100**:391-398.
 19. **Bruchmann A, Roller C, Walther TV, Schafer G, Lehmusvaara S, Visakorpi T, Klocker H, Cato AC, Maddalo D.** 2013. Bcl-2 associated athanogene 5 (Bag5) is overexpressed in prostate cancer and inhibits ER-stress induced apoptosis. *BMC cancer* **13**:96.
 20. **Buchkovich NJ, Maguire TG, Yu Y, Paton AW, Paton JC, Alwine JC.** 2008. Human cytomegalovirus specifically controls the levels of the endoplasmic reticulum chaperone BiP/GRP78, which is required for virion assembly. *Journal of virology* **82**:31-39.
 21. **Burgess SC, Davison TF.** 2002. Identification of the neoplastically transformed cells in Marek's disease herpesvirus-induced lymphomas: recognition by the monoclonal antibody AV37. *Journal of virology* **76**:7276-7292.

22. **Burgess SC, Young JR, Baaten BJ, Hunt L, Ross LN, Parcels MS, Kumar PM, Tregaskes CA, Lee LF, Davison TF.** 2004. Marek's disease is a natural model for lymphomas overexpressing Hodgkin's disease antigen (CD30). *Proceedings of the National Academy of Sciences of the United States of America* **101**:13879-13884.
23. **Burnett HF, Audas TE, Liang G, Lu RR.** 2012. Herpes simplex virus-1 disarms the unfolded protein response in the early stages of infection. *Cell stress & chaperones* **17**:473-483.
24. **Bustin SA.** 2010. Why the need for qPCR publication guidelines?--The case for MIQE. *Methods* **50**:217-226.
25. **Bustin SA, Nolan T.** 2004. Pitfalls of quantitative real-time reverse-transcription polymerase chain reaction. *Journal of biomolecular techniques : JBT* **15**:155-166.
26. **Calnek BW.** 1986. Marek's disease--a model for herpesvirus oncology. *Critical reviews in microbiology* **12**:293-320.
27. **Chen X, Iliopoulos D, Zhang Q, Tang Q, Greenblatt MB, Hatziapostolou M, Lim E, Tam WL, Ni M, Chen Y, Mai J, Shen H, Hu DZ, Adoro S, Hu B, Song M, Tan C, Landis MD, Ferrari M, Shin SJ, Brown M, Chang JC, Liu XS, Glimcher LH.** 2014. XBP1 promotes triple-negative breast cancer by controlling the HIF1alpha pathway. *Nature* **508**:103-107.
28. **Cheng G, Feng Z, He B.** 2005. Herpes simplex virus 1 infection activates the endoplasmic reticulum resident kinase PERK and mediates eIF-2alpha dephosphorylation by the gamma(1)34.5 protein. *Journal of virology* **79**:1379-1388.
29. **Ciofani M, Madar A, Galan C, Sellars M, Mace K, Pauli F, Agarwal A, Huang W, Parkurst CN, Muratet M, Newberry KM, Meadows S, Greenfield A, Yang Y, Jain P, Kirigin FK, Birchmeier C, Wagner EF, Murphy KM, Myers RM, Bonneau R, Littman DR.** 2012. A validated regulatory network for Th17 cell specification. *Cell* **151**:289-303.
30. **Cote-Sierra J, Foucras G, Guo L, Chiodetti L, Young HA, Hu-Li J, Zhu J, Paul WE.** 2004. Interleukin 2 plays a central role in Th2 differentiation. *Proceedings of the National Academy of Sciences of the United States of America* **101**:3880-3885.
31. **Davies MP, Barraclough DL, Stewart C, Joyce KA, Eccles RM, Barraclough R, Rudland PS, Sibson DR.** 2008. Expression and splicing of the unfolded protein response gene XBP-1 are significantly associated with clinical outcome of endocrine-treated breast cancer. *International journal of cancer. Journal international du cancer* **123**:85-88.
32. **Davison F KP.** 2004. Immunity to Marek's disease. In: Davison F, Nair V (eds) *Marek's disease, an evolving problem* **1**:126-139.
33. **de Haro C, Mendez R, Santoyo J.** 1996. The eIF-2alpha kinases and the control of protein synthesis. *FASEB journal : official publication of the Federation of American Societies for Experimental Biology* **10**:1378-1387.

34. **DeLay ML, Turner MJ, Klenk EI, Smith JA, Sowders DP, Colbert RA.** 2009. HLA-B27 misfolding and the unfolded protein response augment interleukin-23 production and are associated with Th17 activation in transgenic rats. *Arthritis and rheumatism* **60**:2633-2643.
35. **Dheda K, Huggett JF, Bustin SA, Johnson MA, Rook G, Zumla A.** 2004. Validation of housekeeping genes for normalizing RNA expression in real-time PCR. *BioTechniques* **37**:112-114, 116, 118-119.
36. **Digby MR, Lowenthal JW.** 1995. Cloning and expression of the chicken interferon-gamma gene. *Journal of interferon & cytokine research : the official journal of the International Society for Interferon and Cytokine Research* **15**:939-945.
37. **Engel AT, Selvaraj RK, Kamil JP, Osterrieder N, Kaufer BB.** 2012. Marek's disease viral interleukin-8 promotes lymphoma formation through targeted recruitment of B cells and CD4+ CD25+ T cells. *Journal of virology* **86**:8536-8545.
38. **Forest T, Barnard S, Baines JD.** 2005. Active intranuclear movement of herpesvirus capsids. *Nature cell biology* **7**:429-431.
39. **Fu Y, Li J, Lee AS.** 2007. GRP78/BiP inhibits endoplasmic reticulum BIK and protects human breast cancer cells against estrogen starvation-induced apoptosis. *Cancer research* **67**:3734-3740.
40. **Fujimoto T, Yoshimatsu K, Watanabe K, Yokomizo H, Otani T, Matsumoto A, Osawa G, Onda M, Ogawa K.** 2007. Overexpression of human X-box binding protein 1 (XBP-1) in colorectal adenomas and adenocarcinomas. *Anticancer research* **27**:127-131.
41. **Garcia-Camacho L, Schat KA, Brooks R, Jr., Bounous DI.** 2003. Early cell-mediated immune responses to Marek's disease virus in two chicken lines with defined major histocompatibility complex antigens. *Veterinary immunology and immunopathology* **95**:145-153.
42. **Gething MJ, Sambrook J.** 1992. Protein folding in the cell. *Nature* **355**:33-45.
43. **Gherardi RK.** 2011. Pathogenic aspects of dermatomyositis, polymyositis and overlap myositis. *Presse medicale* **40**:e209-218.
44. **Gilfillan MC, Noel PJ, Podack ER, Reiner SL, Thompson CB.** 1998. Expression of the costimulatory receptor CD30 is regulated by both CD28 and cytokines. *Journal of immunology* **160**:2180-2187.
45. **Gimeno IM, Witter RL, Cortes AL, Reed WM.** 2011. Replication ability of three highly protective Marek's disease vaccines: implications in lymphoid organ atrophy and protection. *Avian pathology : journal of the W.V.P.A* **40**:573-579.
46. **Goodall JC, Wu C, Zhang Y, McNeill L, Ellis L, Saudek V, Gaston JS.** 2010. Endoplasmic reticulum stress-induced transcription factor, CHOP, is crucial for dendritic cell IL-23 expression. *Proceedings of the National Academy of Sciences of the United States of America* **107**:17698-17703.

47. **Gray MJ, Mhaweche-Fauceglia P, Yoo E, Yang W, Wu E, Lee AS, Lin YG.** 2013. AKT inhibition mitigates GRP78 (glucose-regulated protein) expression and contribution to chemoresistance in endometrial cancers. *International journal of cancer. Journal international du cancer* **133**:21-30.
48. **Greco A, Fester N, Engel AT, Kaufer BB.** 2014. Role of the short telomeric repeat region in Marek's disease virus replication, genomic integration, and lymphomagenesis. *Journal of virology* **88**:14138-14147.
49. **Han J, Back SH, Hur J, Lin Y-H, Gildersleeve R, Shan J, Yuan CL, Krokowski D, Wang S, Hatzoglou M, Kilberg MS, Sartor MA, Kaufman RJ.** 2013. ER-stress-induced transcriptional regulation increases protein synthesis leading to cell death. *Nature cell biology* **15**:481-490.
50. **Haq K, Wootton SK, Barjesteh N, Golovan S, Bendall A, Sharif S.** 2015. Effects of interferon-gamma knockdown on vaccine-induced immunity against Marek's disease in chickens. *Canadian journal of veterinary research = Revue canadienne de recherche veterinaire* **79**:1-7.
51. **Harding HP, Calton M, Urano F, Novoa I, Ron D.** 2002. TRANSCRIPTIONAL AND TRANSLATIONAL CONTROL IN THE MAMMALIAN UNFOLDED PROTEIN RESPONSE. *Annual Review of Cell and Developmental Biology* **18**:575-599.
52. **Hegde NR, Chevalier MS, Wisner TW, Denton MC, Shire K, Frappier L, Johnson DC.** 2006. The role of BiP in endoplasmic reticulum-associated degradation of major histocompatibility complex class I heavy chain induced by cytomegalovirus proteins. *The Journal of biological chemistry* **281**:20910-20919.
53. **Hetz C, Glimcher LH.** 2009. Fine-tuning of the unfolded protein response: Assembling the IRE1alpha interactome. *Molecular cell* **35**:551-561.
54. **Hollien J, Lin JH, Li H, Stevens N, Walter P, Weissman JS.** 2009. Regulated Ire1-dependent decay of messenger RNAs in mammalian cells. *The Journal of cell biology* **186**:323-331.
55. **Hollien J, Weissman JS.** 2006. Decay of endoplasmic reticulum-localized mRNAs during the unfolded protein response. *Science* **313**:104-107.
56. **Hu F, Yu X, Wang H, Zuo D, Guo C, Yi H, Tirosh B, Subject JR, Qiu X, Wang XY.** 2011. ER stress and its regulator X-box-binding protein-1 enhance polyIC-induced innate immune response in dendritic cells. *European journal of immunology* **41**:1086-1097.
57. **Hua Y, White-Gilbertson S, Kellner J, Rachidi S, Usmani SZ, Chiosis G, Depinho R, Li Z, Liu B.** 2013. Molecular chaperone gp96 is a novel therapeutic target of multiple myeloma. *Clinical cancer research : an official journal of the American Association for Cancer Research* **19**:6242-6251.
58. **Huggett J, Dheda K, Bustin S, Zumla A.** 2005. Real-time RT-PCR normalisation; strategies and considerations. *Genes and immunity* **6**:279-284.
59. **Hurtley SM, Helenius A.** 1989. Protein oligomerization in the endoplasmic reticulum. *Annual review of cell biology* **5**:277-307.

60. **Islam A, Cheetham BF, Mahony TJ, Young PL, Walkden-Brown SW.** 2006. Absolute quantitation of Marek's disease virus and Herpesvirus of turkeys in chicken lymphocyte, feather tip and dust samples using real-time PCR. *Journal of virological methods* **132**:127-134.
61. **Isler JA, Skalet AH, Alwine JC.** 2005. Human cytomegalovirus infection activates and regulates the unfolded protein response. *Journal of virology* **79**:6890-6899.
62. **Jarosinski KW, Njaa BL, O'Connell P H, Schat KA.** 2005. Pro-inflammatory responses in chicken spleen and brain tissues after infection with very virulent plus Marek's disease virus. *Viral immunology* **18**:148-161.
63. **Jauhiainen A, Thomsen C, Strombom L, Grundevik P, Andersson C, Danielsson A, Andersson MK, Nerman O, Rorkvist L, Stahlberg A, Aman P.** 2012. Distinct cytoplasmic and nuclear functions of the stress induced protein DDIT3/CHOP/GADD153. *PloS one* **7**:e33208.
64. **Jones D, Brunovskis P, Witter R, Kung HJ.** 1996. Retroviral insertional activation in a herpesvirus: transcriptional activation of US genes by an integrated long terminal repeat in a Marek's disease virus clone. *Journal of virology* **70**:2460-2467.
65. **Jones D, Lee L, Liu JL, Kung HJ, Tillotson JK.** 1992. Marek disease virus encodes a basic-leucine zipper gene resembling the fos/jun oncogenes that is highly expressed in lymphoblastoid tumors. *Proceedings of the National Academy of Sciences of the United States of America* **89**:4042-4046.
66. **Kaiser P, Underwood G, Davison F.** 2003. Differential cytokine responses following Marek's disease virus infection of chickens differing in resistance to Marek's disease. *Journal of virology* **77**:762-768.
67. **Kaufer BB, Jarosinski KW, Osterrieder N.** 2011. Herpesvirus telomeric repeats facilitate genomic integration into host telomeres and mobilization of viral DNA during reactivation. *The Journal of experimental medicine* **208**:605-615.
68. **Kaufman RJ.** 2002. Orchestrating the unfolded protein response in health and disease. *The Journal of clinical investigation* **110**:1389-1398.
69. **Kingham BF, Zelnik V, Kopacek J, Majerciak V, Ney E, Schmidt CJ.** 2001. The genome of herpesvirus of turkeys: comparative analysis with Marek's disease viruses. *The Journal of general virology* **82**:1123-1135.
70. **Klupp BG, Granzow H, Mettenleiter TC.** 2001. Effect of the pseudorabies virus US3 protein on nuclear membrane localization of the UL34 protein and virus egress from the nucleus. *The Journal of general virology* **82**:2363-2371.
71. **Koritzinsky M, Levitin F, van den Beucken T, Rumantir RA, Harding NJ, Chu KC, Boutros PC, Braakman I, Wouters BG.** 2013. Two phases of disulfide bond formation have differing requirements for oxygen. *The Journal of cell biology* **203**:615-627.
72. **Korn T, Bettelli E, Oukka M, Kuchroo VK.** 2009. IL-17 and Th17 Cells. *Annual review of immunology* **27**:485-517.

73. **Kryczek I, Banerjee M, Cheng P, Vatan L, Szeliga W, Wei S, Huang E, Finlayson E, Simeone D, Welling TH, Chang A, Coukos G, Liu R, Zou W.** 2009. Phenotype, distribution, generation, and functional and clinical relevance of Th17 cells in the human tumor environments. *Blood* **114**:1141-1149.
74. **Kryczek I, Wei S, Zou L, Altuwajri S, Szeliga W, Kolls J, Chang A, Zou W.** 2007. Cutting edge: Th17 and regulatory T cell dynamics and the regulation by IL-2 in the tumor microenvironment. *Journal of immunology* **178**:6730-6733.
75. **Kumar S, Buza JJ, Burgess SC.** 2009. Genotype-dependent tumor regression in Marek's disease mediated at the level of tumor immunity. *Cancer microenvironment : official journal of the International Cancer Microenvironment Society* **2**:23-31.
76. **Kung HJ, Xia L, Brunovskis P, Li D, Liu JL, Lee LF.** 2001. Meq: an MDV-specific bZIP transactivator with transforming properties. *Current topics in microbiology and immunology* **255**:245-260.
77. **Lai E, Teodoro T, Volchuk A.** 2007. Endoplasmic reticulum stress: signaling the unfolded protein response. *Physiology* **22**:193-201.
78. **Lee AH, Iwakoshi NN, Glimcher LH.** 2003. XBP-1 regulates a subset of endoplasmic reticulum resident chaperone genes in the unfolded protein response. *Molecular and cellular biology* **23**:7448-7459.
79. **Lee AS.** 2014. Glucose-regulated proteins in cancer: molecular mechanisms and therapeutic potential. *Nature reviews. Cancer* **14**:263-276.
80. **Lee DY, Sugden B.** 2008. The LMP1 oncogene of EBV activates PERK and the unfolded protein response to drive its own synthesis. *Blood* **111**:2280-2289.
81. **Lenna S, Farina AG, Martyanov V, Christmann RB, Wood TA, Farber HW, Scorza R, Whitfield ML, Lafyatis R, Trojanowska M.** 2013. Increased expression of endoplasmic reticulum stress and unfolded protein response genes in peripheral blood mononuclear cells from patients with limited cutaneous systemic sclerosis and pulmonary arterial hypertension. *Arthritis and rheumatism* **65**:1357-1366.
82. **Levy AM, Gilad O, Xia L, Izumiya Y, Choi J, Tsalenko A, Yakhini Z, Witter R, Lee L, Cardona CJ, Kung HJ.** 2005. Marek's disease virus Meq transforms chicken cells via the v-Jun transcriptional cascade: a converging transforming pathway for avian oncoviruses. *Proceedings of the National Academy of Sciences of the United States of America* **102**:14831-14836.
83. **Levy AM, Izumiya Y, Brunovskis P, Xia L, Parcels MS, Reddy SM, Lee L, Chen HW, Kung HJ.** 2003. Characterization of the chromosomal binding sites and dimerization partners of the viral oncoprotein Meq in Marek's disease virus-transformed T cells. *Journal of virology* **77**:12841-12851.
84. **Li Y, Schwabe RF, DeVries-Seimon T, Yao PM, Gerbod-Giannone MC, Tall AR, Davis RJ, Flavell R, Brenner DA, Tabas I.** 2005. Free cholesterol-loaded macrophages are an abundant source of tumor necrosis factor-alpha and

- interleukin-6: model of NF-kappaB- and map kinase-dependent inflammation in advanced atherosclerosis. *The Journal of biological chemistry* **280**:21763-21772.
85. **Li Z, Li Z.** 2012. Glucose regulated protein 78: a critical link between tumor microenvironment and cancer hallmarks. *Biochimica et biophysica acta* **1826**:13-22.
 86. **Lian L, Qu LJ, Sun HY, Chen YM, Lamont SJ, Liu CJ, Yang N.** 2012. Gene expression analysis of host spleen responses to Marek's disease virus infection at late tumor transformation phase. *Poultry science* **91**:2130-2138.
 87. **Liao W, Lin JX, Wang L, Li P, Leonard WJ.** 2011. Modulation of cytokine receptors by IL-2 broadly regulates differentiation into helper T cell lineages. *Nature immunology* **12**:551-559.
 88. **Lin JH, Li H, Yasumura D, Cohen HR, Zhang C, Panning B, Shokat KM, Lavail MM, Walter P.** 2007. IRE1 signaling affects cell fate during the unfolded protein response. *Science* **318**:944-949.
 89. **Liu B, Staron M, Hong F, Wu BX, Sun S, Morales C, Crosson CE, Tomlinson S, Kim I, Wu D, Li Z.** 2013. Essential roles of grp94 in gut homeostasis via chaperoning canonical Wnt pathway. *Proceedings of the National Academy of Sciences of the United States of America* **110**:6877-6882.
 90. **Liu JL, Lin SF, Xia L, Brunovskis P, Li D, Davidson I, Lee LF, Kung HJ.** 1999. MEQ and V-IL8: cellular genes in disguise? *Acta virologica* **43**:94-101.
 91. **Liu JL, Ye Y, Lee LF, Kung HJ.** 1998. Transforming potential of the herpesvirus oncoprotein MEQ: morphological transformation, serum-independent growth, and inhibition of apoptosis. *Journal of virology* **72**:388-395.
 92. **Liu R, Li X, Gao W, Zhou Y, Wey S, Mitra SK, Krasnoperov V, Dong D, Liu S, Li D, Zhu G, Louie S, Conti PS, Li Z, Lee AS, Gill PS.** 2013. Monoclonal antibody against cell surface GRP78 as a novel agent in suppressing PI3K/AKT signaling, tumor growth, and metastasis. *Clinical cancer research : an official journal of the American Association for Cancer Research* **19**:6802-6811.
 93. **Luo B, Lee AS.** 2013. The critical roles of endoplasmic reticulum chaperones and unfolded protein response in tumorigenesis and anticancer therapies. *Oncogene* **32**:805-818.
 94. **Lupiani B, Lee LF, Cui X, Gimeno I, Anderson A, Morgan RW, Silva RF, Witter RL, Kung HJ, Reddy SM.** 2004. Marek's disease virus-encoded Meq gene is involved in transformation of lymphocytes but is dispensable for replication. *Proceedings of the National Academy of Sciences of the United States of America* **101**:11815-11820.
 95. **Lussignol M, Queval C, Bernet-Camard MF, Cotte-Laffitte J, Beau I, Codogno P, Esclatine A.** 2013. The herpes simplex virus 1 Us11 protein

- inhibits autophagy through its interaction with the protein kinase PKR. *Journal of virology* **87**:859-871.
96. **Ma Y, Brewer JW, Diehl JA, Hendershot LM.** 2002. Two distinct stress signaling pathways converge upon the CHOP promoter during the mammalian unfolded protein response. *Journal of molecular biology* **318**:1351-1365.
 97. **Ma Y, Hendershot LM.** 2004. ER chaperone functions during normal and stress conditions. *Journal of chemical neuroanatomy* **28**:51-65.
 98. **Mackay IM, Arden KE, Nitsche A.** 2002. Real-time PCR in virology. *Nucleic acids research* **30**:1292-1305.
 99. **Maestre L, Tooze R, Canamero M, Montes-Moreno S, Ramos R, Doody G, Boll M, Barrans S, Baena S, Piris MA, Roncador G.** 2009. Expression pattern of XBP1(S) in human B-cell lymphomas. *Haematologica* **94**:419-422.
 100. **Malhotra JD, Kaufman RJ.** 2007. The endoplasmic reticulum and the unfolded protein response. *Seminars in cell & developmental biology* **18**:716-731.
 101. **Marek J.** 1907. Multiple Nervenentzündung (Polyneuritis). bei Hühnern. *Dtsch. Tierärztl. Wochenschr.* **15**,417–421.
 102. **Martinon F, Chen X, Lee AH, Glimcher LH.** 2010. TLR activation of the transcription factor XBP1 regulates innate immune responses in macrophages. *Nature immunology* **11**:411-418.
 103. **Maytin EV, Ubeda M, Lin JC, Habener JF.** 2001. Stress-inducible transcription factor CHOP/gadd153 induces apoptosis in mammalian cells via p38 kinase-dependent and -independent mechanisms. *Experimental cell research* **267**:193-204.
 104. **Mielants H, Veys EM, Cuvelier C, de Vos M.** 1988. Ileocolonoscopy findings in seronegative spondylarthropathies. *British journal of rheumatology* **27 Suppl 2**:95-105.
 105. **Miyahara Y, Odunsi K, Chen W, Peng G, Matsuzaki J, Wang RF.** 2008. Generation and regulation of human CD4+ IL-17-producing T cells in ovarian cancer. *Proceedings of the National Academy of Sciences of the United States of America* **105**:15505-15510.
 106. **Morgan RW, Sofer L, Anderson AS, Bernberg EL, Cui J, Burnside J.** 2001. Induction of host gene expression following infection of chicken embryo fibroblasts with oncogenic Marek's disease virus. *Journal of virology* **75**:533-539.
 107. **Morimura T, Hattori M, Ohashi K, Sugimoto C, Onuma M.** 1995. Immunomodulation of peripheral T cells in chickens infected with Marek's disease virus: involvement in immunosuppression. *The Journal of general virology* **76 (Pt 12)**:2979-2985.
 108. **Morimura T, Ohashi K, Kon Y, Hattori M, Sugimoto C, Onuma M.** 1996. Apoptosis and CD8-down-regulation in the thymus of chickens infected with Marek's disease virus. *Archives of virology* **141**:2243-2249.

109. **Morimura T, Ohashi K, Kon Y, Hattori M, Sugimoto C, Onuma M.** 1997. Apoptosis in peripheral CD4+T cells and thymocytes by Marek's disease virus-infection. *Leukemia* **11 Suppl 3**:206-208.
110. **Mulvey M, Arias C, Mohr I.** 2007. Maintenance of endoplasmic reticulum (ER) homeostasis in herpes simplex virus type 1-infected cells through the association of a viral glycoprotein with PERK, a cellular ER stress sensor. *Journal of virology* **81**:3377-3390.
111. **Murata S, Hashiguchi T, Hayashi Y, Yamamoto Y, Matsuyama-Kato A, Takasaki S, Isezaki M, Onuma M, Konnai S, Ohashi K.** 2013. Characterization of Meq proteins from field isolates of Marek's disease virus in Japan. *Infection, genetics and evolution : journal of molecular epidemiology and evolutionary genetics in infectious diseases* **16**:137-143.
112. **Murata S, Okada T, Kano R, Hayashi Y, Hashiguchi T, Onuma M, Konnai S, Ohashi K.** 2011. Analysis of transcriptional activities of the Meq proteins present in highly virulent Marek's disease virus strains, RB1B and Md5. *Virus genes* **43**:66-71.
113. **Murugaiyan G, Saha B.** 2009. Protumor vs antitumor functions of IL-17. *Journal of immunology* **183**:4169-4175.
114. **Mwangi WN, Smith LP, Baigent SJ, Beal RK, Nair V, Smith AL.** 2011. Clonal Structure of Rapid-Onset MDV-Driven CD4+ Lymphomas and Responding CD8+ T Cells. *PLoS Pathog* **7**:e1001337.
115. **Nagaraju K, Casciola-Rosen L, Lundberg I, Rawat R, Cutting S, Thapliyal R, Chang J, Dwivedi S, Mitsak M, Chen YW, Plotz P, Rosen A, Hoffman E, Raben N.** 2005. Activation of the endoplasmic reticulum stress response in autoimmune myositis: potential role in muscle fiber damage and dysfunction. *Arthritis and rheumatism* **52**:1824-1835.
116. **Ni M, Zhang Y, Lee AS.** 2011. Beyond the endoplasmic reticulum: atypical GRP78 in cell viability, signalling and therapeutic targeting. *The Biochemical journal* **434**:181-188.
117. **Nishitoh H, Matsuzawa A, Tobiume K, Saegusa K, Takeda K, Inoue K, Hori S, Kakizuka A, Ichijo H.** 2002. ASK1 is essential for endoplasmic reticulum stress-induced neuronal cell death triggered by expanded polyglutamine repeats. *Genes & development* **16**:1345-1355.
118. **Oida T, Weiner HL.** 2010. TGF-beta induces surface LAP expression on murine CD4 T cells independent of Foxp3 induction. *PloS one* **5**:e15523.
119. **Okada K, Tanaka Y, Murakami K, Chiba S, Morimura T, Hattori M, Goryo M, Onuma M.** 1997. Phenotype analysis of lymphoid cells in Marek's disease of CD4(+) or CD8(+) T-cell-deficient chickens: Occurrence of double negative T-cell tumour. *Avian pathology : journal of the W.V.P.A* **26**:525-534.
120. **Pappenheimer AW, Dunn, L. C. & Seidlin, S. M.** 1929b. Studies on fowl paralysis (Neurolymphomatosis gallinarum). II. Transmission experiments. *J. Exp. Med.* **49**: 87-102

121. **Parcells M, Burgess S.** 2008. Immunological aspects of Marek's disease virus (MDV)-induced lymphoma progression, p. 169-191. *In* Kaiser H, Nasir A (ed.), Selected Aspects of Cancer Progression: Metastasis, Apoptosis and Immune Response, vol. 11. Springer Netherlands.
122. **Parcells MS, Lin SF, Dienglewicz RL, Majerciak V, Robinson DR, Chen HC, Wu Z, Dubyak GR, Brunovskis P, Hunt HD, Lee LF, Kung HJ.** 2001. Marek's disease virus (MDV) encodes an interleukin-8 homolog (vIL-8): characterization of the vIL-8 protein and a vIL-8 deletion mutant MDV. *Journal of virology* **75**:5159-5173.
123. **Pereira ER, Frudd K, Awad W, Hendershot LM.** 2014. Endoplasmic reticulum (ER) stress and hypoxia response pathways interact to potentiate hypoxia-inducible factor 1 (HIF-1) transcriptional activity on targets like vascular endothelial growth factor (VEGF). *The Journal of biological chemistry* **289**:3352-3364.
124. **Peters W.** 2014. The effect of mutations in the Meq oncoprotein of Marek's disease virus (MDV) on lymphomas composition
by Peters, Wachen, M.S., UNIVERSITY OF DELAWARE, 2014, 92 pages; 1567819.
125. **Pfaffenbach KT, Pong M, Morgan TE, Wang H, Ott K, Zhou B, Longo VD, Lee AS.** 2012. GRP78/BiP is a novel downstream target of IGF-1 receptor mediated signaling. *Journal of cellular physiology* **227**:3803-3811.
126. **Purves FC, Spector D, Roizman B.** 1991. The herpes simplex virus 1 protein kinase encoded by the US3 gene mediates posttranslational modification of the phosphoprotein encoded by the UL34 gene. *Journal of virology* **65**:5757-5764.
127. **Radonic A, Thulke S, Bae HG, Muller MA, Siegert W, Nitsche A.** 2005. Reference gene selection for quantitative real-time PCR analysis in virus infected cells: SARS corona virus, Yellow fever virus, Human Herpesvirus-6, Camelpox virus and Cytomegalovirus infections. *Virology journal* **2**:7.
128. **Reddy RK, Lu J, Lee AS.** 1999. The endoplasmic reticulum chaperone glycoprotein GRP94 with Ca(2+)-binding and antiapoptotic properties is a novel proteolytic target of calpain during etoposide-induced apoptosis. *The Journal of biological chemistry* **274**:28476-28483.
129. **Reddy RK, Mao C, Baumeister P, Austin RC, Kaufman RJ, Lee AS.** 2003. Endoplasmic reticulum chaperone protein GRP78 protects cells from apoptosis induced by topoisomerase inhibitors: role of ATP binding site in suppression of caspase-7 activation. *The Journal of biological chemistry* **278**:20915-20924.
130. **Reinke AW, Grigoryan G, Keating AE.** 2010. Identification of bZIP interaction partners of viral proteins HBZ, MEQ, BZLF1, and K-bZIP using coiled-coil arrays. *Biochemistry* **49**:1985-1997.
131. **Reynolds AE, Wills EG, Roller RJ, Ryckman BJ, Baines JD.** 2002. Ultrastructural localization of the herpes simplex virus type 1 UL31, UL34, and US3 proteins suggests specific roles in primary envelopment and egress of nucleocapsids. *Journal of virology* **76**:8939-8952.

132. **Richerieux N, Blondeau C, Wiedemann A, Remy S, Vautherot JF, Denesvre C.** 2012. Rho-ROCK and Rac-PAK signaling pathways have opposing effects on the cell-to-cell spread of Marek's Disease Virus. *PloS one* **7**:e44072.
133. **Rocha EP.** 2004. The replication-related organization of bacterial genomes. *Microbiology* **150**:1609-1627.
134. **Ryckman BJ, Roller RJ.** 2004. Herpes simplex virus type 1 primary envelopment: UL34 protein modification and the US3-UL34 catalytic relationship. *Journal of virology* **78**:399-412.
135. **Ryder CB, McColl K, Distelhorst CW.** 2013. Acidosis blocks CCAAT/enhancer-binding protein homologous protein (CHOP)- and c-Jun-mediated induction of p53-upregulated mediator of apoptosis (PUMA) during amino acid starvation. *Biochemical and biophysical research communications* **430**:1283-1288.
136. **Schardt JA, Mueller BU, Pabst T.** 2011. Activation of the unfolded protein response in human acute myeloid leukemia. *Methods in enzymology* **489**:227-243.
137. **Schat KA, Chen CL, Calnek BW, Char D.** 1991. Transformation of T-lymphocyte subsets by Marek's disease herpesvirus. *Journal of virology* **65**:1408-1413.
138. **Schermuly J, Greco A, Hartle S, Osterrieder N, Kaufer BB, Kaspers B.** 2015. In vitro model for lytic replication, latency, and transformation of an oncogenic alphaherpesvirus. *Proceedings of the National Academy of Sciences of the United States of America*.
139. **Schmittgen TD, Zakrajsek BA.** 2000. Effect of experimental treatment on housekeeping gene expression: validation by real-time, quantitative RT-PCR. *Journal of biochemical and biophysical methods* **46**:69-81.
140. **Schroder M, Kaufman RJ.** 2005. The mammalian unfolded protein response. *Annual review of biochemistry* **74**:739-789.
141. **Schubert U, Anton LC, Gibbs J, Norbury CC, Yewdell JW, Bennink JR.** 2000. Rapid degradation of a large fraction of newly synthesized proteins by proteasomes. *Nature* **404**:770-774.
142. **Schumacher D, McKinney C, Kaufer BB, Osterrieder N.** 2008. Enzymatically inactive U(S)3 protein kinase of Marek's disease virus (MDV) is capable of depolymerizing F-actin but results in accumulation of virions in perinuclear invaginations and reduced virus growth. *Virology* **375**:37-47.
143. **Schumacher D, Tischer BK, Trapp S, Osterrieder N.** 2005. The protein encoded by the US3 orthologue of Marek's disease virus is required for efficient de-envelopment of perinuclear virions and involved in actin stress fiber breakdown. *Journal of virology* **79**:3987-3997.
144. **Sfanos KS, Bruno TC, Maris CH, Xu L, Thoburn CJ, DeMarzo AM, Meeker AK, Isaacs WB, Drake CG.** 2008. Phenotypic analysis of prostate-infiltrating lymphocytes reveals TH17 and Treg skewing. *Clinical cancer*

- research : an official journal of the American Association for Cancer Research **14**:3254-3261.
145. **Shack LA, Buza JJ, Burgess SC.** 2008. The neoplastically transformed (CD30hi) Marek's disease lymphoma cell phenotype most closely resembles T-regulatory cells. *Cancer immunology, immunotherapy* : CII **57**:1253-1262.
 146. **Shamblin CE, Greene N, Arumugaswami V, Dienglewicz RL, Parcels MS.** 2004. Comparative analysis of Marek's disease virus (MDV) glycoprotein-, lytic antigen pp38- and transformation antigen Meq-encoding genes: association of meq mutations with MDVs of high virulence. *Veterinary microbiology* **102**:147-167.
 147. **Shu CW, Sun FC, Cho JH, Lin CC, Liu PF, Chen PY, Chang MD, Fu HW, Lai YK.** 2008. GRP78 and Raf-1 cooperatively confer resistance to endoplasmic reticulum stress-induced apoptosis. *Journal of cellular physiology* **215**:627-635.
 148. **Smith JA.** 2014. A new paradigm: innate immune sensing of viruses via the unfolded protein response. *Frontiers in microbiology* **5**:222.
 149. **Smith JA, Turner MJ, DeLay ML, Klenk EI, Sowders DP, Colbert RA.** 2008. Endoplasmic reticulum stress and the unfolded protein response are linked to synergistic IFN-beta induction via X-box binding protein 1. *European journal of immunology* **38**:1194-1203.
 150. **Stahlberg A, Kubista M, Pfaffl M.** 2004. Comparison of reverse transcriptases in gene expression analysis. *Clinical chemistry* **50**:1678-1680.
 151. **Stone KR, Smith RE, Joklik WK.** 1974. Changes in membrane polypeptides that occur when chick embryo fibroblasts and NRK cells are transformed with avian sarcoma viruses. *Virology* **58**:86-100.
 152. **Stritesky GL, Yeh N, Kaplan MH.** 2008. IL-23 promotes maintenance but not commitment to the Th17 lineage. *Journal of immunology* **181**:5948-5955.
 153. **Sun X, Yamada H, Shibata K, Muta H, Tani K, Podack ER, Yoshikai Y.** 2010. CD30 ligand/CD30 plays a critical role in Th17 differentiation in mice. *Journal of immunology* **185**:2222-2230.
 154. **Suto A, Kashiwakuma D, Kagami S, Hirose K, Watanabe N, Yokote K, Saito Y, Nakayama T, Grusby MJ, Iwamoto I, Nakajima H.** 2008. Development and characterization of IL-21-producing CD4+ T cells. *The Journal of experimental medicine* **205**:1369-1379.
 155. **Talaat AM, Howard ST, Hale Wt, Lyons R, Garner H, Johnston SA.** 2002. Genomic DNA standards for gene expression profiling in *Mycobacterium tuberculosis*. *Nucleic acids research* **30**:e104.
 156. **Talloczy Z, Virgin HWt, Levine B.** 2006. PKR-dependent autophagic degradation of herpes simplex virus type 1. *Autophagy* **2**:24-29.
 157. **Tam AB, Mercado EL, Hoffmann A, Niwa M.** 2012. ER stress activates NF-kappaB by integrating functions of basal IKK activity, IRE1 and PERK. *PLoS one* **7**:e45078.

158. **Tavlarides-Hontz P, Kumar PM, Amortegui JR, Osterrieder N, Parcels MS.** 2009. A deletion within glycoprotein L of Marek's disease virus (MDV) field isolates correlates with a decrease in bivalent MDV vaccine efficacy in contact-exposed chickens. *Avian diseases* **53**:287-296.
159. **Tavlarides-Hontz P, Kumar PM, Amortegui JR, Osterrieder N, Parcels MS.** 2009. A Deletion within Glycoprotein L of Marek's Disease Virus (MDV) Field Isolates Correlates with A Decrease in Bivalent MDV Vaccine Efficacy in Contact-exposed Chickens. *Avian Diseases Digest* **4**:e15-e15.
160. **Tay KH, Luan Q, Croft A, Jiang CC, Jin L, Zhang XD, Tseng HY.** 2014. Sustained IRE1 and ATF6 signaling is important for survival of melanoma cells undergoing ER stress. *Cellular signalling* **26**:287-294.
161. **Thellin O, Zorzi W, Lakaye B, De Borman B, Coumans B, Hennen G, Grisar T, Igout A, Heinen E.** 1999. Housekeeping genes as internal standards: use and limits. *Journal of biotechnology* **75**:291-295.
162. **Turner MJ, Sowders DP, DeLay ML, Mohapatra R, Bai S, Smith JA, Brandewie JR, Taurog JD, Colbert RA.** 2005. HLA-B27 misfolding in transgenic rats is associated with activation of the unfolded protein response. *Journal of immunology* **175**:2438-2448.
163. **Ubeda M, Vallejo M, Habener JF.** 1999. CHOP enhancement of gene transcription by interactions with Jun/Fos AP-1 complex proteins. *Molecular and cellular biology* **19**:7589-7599.
164. **Urano F, Wang X, Bertolotti A, Zhang Y, Chung P, Harding HP, Ron D.** 2000. Coupling of stress in the ER to activation of JNK protein kinases by transmembrane protein kinase IRE1. *Science* **287**:664-666.
165. **van Huizen R, Martindale JL, Gorospe M, Holbrook NJ.** 2003. P58IPK, a novel endoplasmic reticulum stress-inducible protein and potential negative regulator of eIF2alpha signaling. *The Journal of biological chemistry* **278**:15558-15564.
166. **Vattem KM, Wek RC.** 2004. Reinitiation involving upstream ORFs regulates ATF4 mRNA translation in mammalian cells. *Proceedings of the National Academy of Sciences of the United States of America* **101**:11269-11274.
167. **Wanderling S, Simen BB, Ostrovsky O, Ahmed NT, Vogen SM, Gidalevitz T, Argon Y.** 2007. GRP94 is essential for mesoderm induction and muscle development because it regulates insulin-like growth factor secretion. *Molecular biology of the cell* **18**:3764-3775.
168. **Watson S, Mercier S, Bye C, Wilkinson J, Cunningham AL, Harman AN.** 2007. Determination of suitable housekeeping genes for normalisation of quantitative real time PCR analysis of cells infected with human immunodeficiency virus and herpes viruses. *Virology journal* **4**:130.
169. **Woehlbier U, Hetz C.** 2011. Modulating stress responses by the UPRosome: a matter of life and death. *Trends in biochemical sciences* **36**:329-337.
170. **Xie Q, Anderson AS, Morgan RW.** 1996. Marek's disease virus (MDV) ICP4, pp38, and meq genes are involved in the maintenance of transformation

- of MDCC-MSB1 MDV-transformed lymphoblastoid cells. *Journal of virology* **70**:1125-1131.
171. **Xing Z, Schat KA.** 2000. Expression of cytokine genes in Marek's disease virus-infected chickens and chicken embryo fibroblast cultures. *Immunology* **100**:70-76.
 172. **Xuan B, Qian Z, Torigoi E, Yu D.** 2009. Human cytomegalovirus protein pUL38 induces ATF4 expression, inhibits persistent JNK phosphorylation, and suppresses endoplasmic reticulum stress-induced cell death. *Journal of virology* **83**:3463-3474.
 173. **Ye J, Rawson RB, Komuro R, Chen X, Dave UP, Prywes R, Brown MS, Goldstein JL.** 2000. ER stress induces cleavage of membrane-bound ATF6 by the same proteases that process SREBPs. *Molecular cell* **6**:1355-1364.
 174. **Yeung BH, Kwan BW, He QY, Lee AS, Liu J, Wong AS.** 2008. Glucose-regulated protein 78 as a novel effector of BRCA1 for inhibiting stress-induced apoptosis. *Oncogene* **27**:6782-6789.
 175. **Yoshida H, Matsui T, Yamamoto A, Okada T, Mori K.** 2001. XBP1 mRNA is induced by ATF6 and spliced by IRE1 in response to ER stress to produce a highly active transcription factor. *Cell* **107**:881-891.
 176. **Zeng L, Liu YP, Sha H, Chen H, Qi L, Smith JA.** 2010. XBP-1 couples endoplasmic reticulum stress to augmented IFN-beta induction via a cis-acting enhancer in macrophages. *Journal of immunology* **185**:2324-2330.
 177. **Zhai L, Kita K, Wano C, Wu Y, Sugaya S, Suzuki N.** 2005. Decreased cell survival and DNA repair capacity after UVC irradiation in association with down-regulation of GRP78/BiP in human R5a cells. *Experimental cell research* **305**:244-252.
 178. **Zhang Y, Liu R, Ni M, Gill P, Lee AS.** 2010. Cell surface relocalization of the endoplasmic reticulum chaperone and unfolded protein response regulator GRP78/BiP. *The Journal of biological chemistry* **285**:15065-15075.
 179. **Zhang Y, Tseng CC, Tsai YL, Fu X, Schiff R, Lee AS.** 2013. Cancer cells resistant to therapy promote cell surface relocalization of GRP78 which complexes with PI3K and enhances PI(3,4,5)P3 production. *PloS one* **8**:e80071.
 180. **Zhao Y, Kurian D, Xu H, Petherbridge L, Smith LP, Hunt L, Nair V.** 2009. Interaction of Marek's disease virus oncoprotein Meq with heat-shock protein 70 in lymphoid tumour cells. *The Journal of general virology* **90**:2201-2208.
 181. **Zhou H, Zhang Y, Fu Y, Chan L, Lee AS.** 2011. Novel mechanism of anti-apoptotic function of 78-kDa glucose-regulated protein (GRP78): endocrine resistance factor in breast cancer, through release of B-cell lymphoma 2 (BCL-2) from BCL-2-interacting killer (BIK). *The Journal of biological chemistry* **286**:25687-25696.
 182. **Zhu X, Mulcahy LA, Mohammed RA, Lee AH, Franks HA, Kilpatrick L, Yilmazer A, Paish EC, Ellis IO, Patel PM, Jackson AM.** 2008. IL-17

expression by breast-cancer-associated macrophages: IL-17 promotes
invasiveness of breast cancer cell lines. Breast cancer research : BCR **10**:R95.

Appendix A

ALIGNMENT OF XBP1 SEQUENCES OF DIFFERENT SPECIES

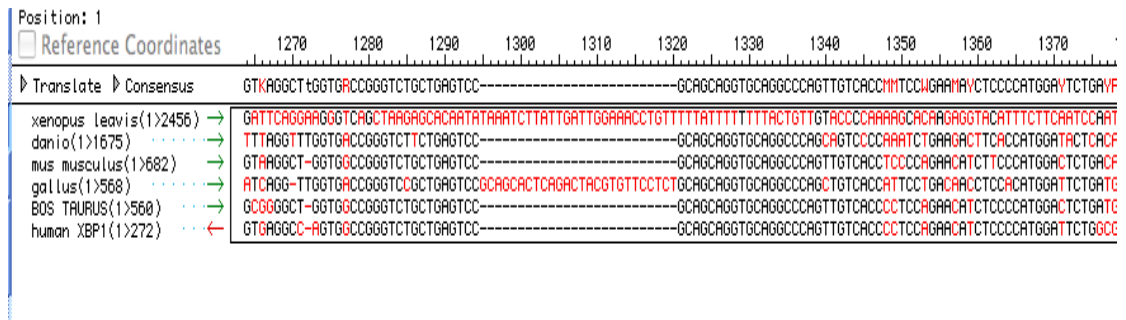


Figure A1: Above figure shows alignment of XBP1 genomic sequences from different species (Xenopus leavis, Danio rerio, Mus musculus, Gallus gallus, Bos Taurus and Homo sapiens) using laser gene software. A 26nt spliced fragment is indicated by dotted line from nucleotide positions 1205-1320.

Appendix B

PRIMER SEQUENCES USED IN THE STUDY

GENE	Tm	Forward primer	Reverse primer	REFERENCE
UB	55	GGGATGCAGATCTTCGTGAAA	CTTGCCAGCAAAGATCAACCTT	18272235
β actin	58	CACAGATCATGTTTGAGACCTT	CATCACAATACCAGTGGTACG	18272235
G6PDH	65	CGGGAACCAAATGCACCTCGT	CGCTGCCGTAGAGGTATGGGA	18272235
GAPDH	55	GGAGTCCACTGGTGTCTTCA	AGCACACCCTTCAGATGAG	This study
PPIB	55	GAGAAAGGGTTCGGCTTCA	GAGAAAGGGTTCGGCTTCA	This study
IL-10	58	GAGCTGAGGGTGAAGTTGAGGAA	CTTTGACACAGACTGGCAGCCAAA	This study
IFN- γ	58	AGATGTAGCTGACGGTGGACCTAT	GATGTGCGGCTTTGACTTGTCAGT	This study
IL-4	58	CTCAACATGCGTCAGCTCCTGAAT	ATTGAAGTAGTGTTCCTGTGCC	This study
IL-17	58	CAAGAAAGCAGATGCTGGATGCCT	CAAGGGTCACTTTGGTATCCTGGT	This study
IL-21	58	CTGTAACCTGCTTCCAGAATGGCA	AGTGCTCTTCAGAGACTGGGAGAA	This study
18S RNA	55	TCAGATACCGTCGTAGTTCC	TCCGTC AATTCCTTTAAGTT	This study
28S RNA	58	GGTATGGGCCGACGCT	CCGATGCCGACGCTCAT	This study
IL-2	58	TCTGCAGTGTTACCTGGGAGAAGT	ACTTCCGGTGTGATTTAGACCCGT	This study
TGFB2	58	TGCCATCCCACCAAGCTATTACAG	GCCTTCACCAAGTTGGACGCATTT	This study
T-bet/TBX21	58	AGGAGGTTTCCTTTGGGAAGCTGA	TGGTTGGTACTTGTGCAGCGACT	This study
IL-6	58	AAGAAGTTCACCGTGTGCGAGAAC	TGGAGAGCTTCGTCAGGCATTTCT	This study
XBP(U)	58	CAGCACTCAGACTACGTGTTCTCTG	CACATGGATTCTGATGGCAG	This study
XBP(S)	58	GCTGAGTCCGCAGCAGG	CACATGGATTCTGATGGCAG	This study
BiP	58	TGTAGCCTATGGTGCAGCTGTTC A	ATGCCAAGTGTCAGAGGACACACA	This study
EDEM	58	ATGACAACGAAGTCTGCACATGG	TGCTGTTGGAGGAACTCCCTTCT	This study
GRP94	58	CTGAGAAGTTTGCCTTTCAAGCAG	GCTCCTCATTACCAGCAAGAGCAT	This study
ATF4	58	CAATTGGCTCGCTGTGGACAGTTT	ACGGTGGCTTCAGATGTTCCATA	This study
meq	58	TCGATCTTTCTCTCGGGTGCACCT	TCCAGCTTCTGTTTCTCTCTCTCA	This study

Appendix C

ANIMAL CARE AND USE COMPLIANCE

The animal use in this study was approved under the Ag Animal Care and Use Committee (AACUC) blanket Vaccine Trial protocol: (22) 04-15-10a. Further, this trial was filed under the one-page form marked by the date: 01-07-12.